CHAPTER 8

Utilization of Three-dimensional Imaging Technology to Enhance Maxillofacial Surgical Applications

Scott D. Ganz, DMD

INTRODUCTION

The evolution in sophisticated diagnostic imaging modalities and associated software applications continues to impact the specialty of oral and maxillofacial surgery. The advent of computed tomography (CT) in dentistry began in the late 1980s with the use of medical-grade machines located in major hospitals or radiology centers. Patients were referred for CT scans to achieve a level of diagnosis beyond the scope of conventional two-dimensional panoramic or periodical radiography available in most dental offices. As computing power increased, the ability to move from two-dimensional to three-dimensional data marked the beginning of a new and exciting area in diagnostic imaging, paving the way for the development and adoption of interactive treatment planning software to help interpret the massive amount of anatomic data. The information gained from a CT scan allowed the clinician to appreciate the "reality of anatomy" for each patient presentation—yielding views of structures aided by advances in data processing power of the computer-driven technology. As dental implants increased in popularity as tooth replacements, the accurate assessment of patient anatomy and collaboration between restorative clinician and surgeon became more critical as determinants of successful outcomes. CT technology and interactive treatment planning software applications helped bridge the communication gap between all members of the implant team, while appreciably removing the guesswork from the process.

Despite all of the benefits of three-dimensional CT scan data, the actual use of the technology was quite limited due to several barriers including cost of the scan, proximity of the radiology center, and lack of proper training in interpretive three-dimensional diagnostics. Recently, a new family of imaging machines was introduced with cone beam computed tomography (CBCT) technology, which offered several immediate benefits for dental applications by helping to remove many of the barriers associated with the imaging modality. CBCT machines are far less costly than a medical-grade CT machine, can offer excellent image quality at a fraction of the radiation dose to the patient, and are small enough to fit into a dental office. Therefore, in the author's opinion, dental applications of three-dimensional imaging has become one of the most significant developments that will have the most impact on how surgical and restorative procedures are planned, communicated, and executed for years to come. As computing processing power, graphics emulations, and display screens continue to dramatically improve, the actual use of the techniques and concepts presented will be ultimately limited by the clinician's imagination. Regardless of the enormous benefits of this technology, there are risks

associated with even low dose radiation exposure. Therefore clinicians should be responsible when utilizing CBCT or CT in adhering to the ALARA principle (As Low As Reasonably Achievable) for each of our patients. The goal of this chapter is to illustrate how this technology can be applied for a variety of different clinical presentations.

Whether using standard CT or CBCT, the scan data requires further processing so that it can be visualized on the computer display. It is not the intent of this chapter to review the technical aspects of this process, as it is the application of the technology that is most rewarding for both clinician and patient. If the patient is referred to a radiology center, the data will be provided on a CD-type disk, with a self-contained viewing software. If an in-office CBCT machine is used, the data will be processed and viewed on a computer workstation. Regardless of how the data are acquired, the software will produce four basic views: the axial, the panoramic, the three-dimensional reconstruction, and the cross-sectional views (Figure 8-1). These four image types are the building blocks for analyzing data, formulating an accurate diagnosis, communicating with clinical teammates, educating the patient, formulating a definitive plan, and properly executing the plan. The key to the process is how each of these images can be utilized through direct interaction such as changing the gray scale, scrolling through the various slices, or simulating implant placement with sophisticated planning tools.

The image acquisition process can be limited by the type of machine used and the size of the data collection sensor. These differences can affect the field of view (FOV). A large FOV machine allows for inspection of the entire maxillofacial complex as displayed in a variety of different formats for diagnostic accuracy (Figure 8-2). An example of the diversity of how data can be displayed is found in the temporomandibular joint (TMJ) view, in which the software automatically generates a series of interactive images focusing on the anatomic landmarks for both the left and the right condyles (Figure 8-3). Various third-party interactive treatment planning software can manipulate the CT/CBCT data in an ever-expanding array of capabilities to facilitate the diagnosis, treatment planning phase, and surgical intervention. The use in maxillofacial surgical procedures includes, but is not limited to, impacted teeth, implant placement, block and particulate bone grafting, orthognathic procedures, distraction osteogenesis, TMJ dysfunction, sinus augmentation, and many others. Each of these procedures can be enhanced through the application of three-dimensional imaging technologies. The following clinical presentations demonstrate how new three-dimensional tools can be applied.

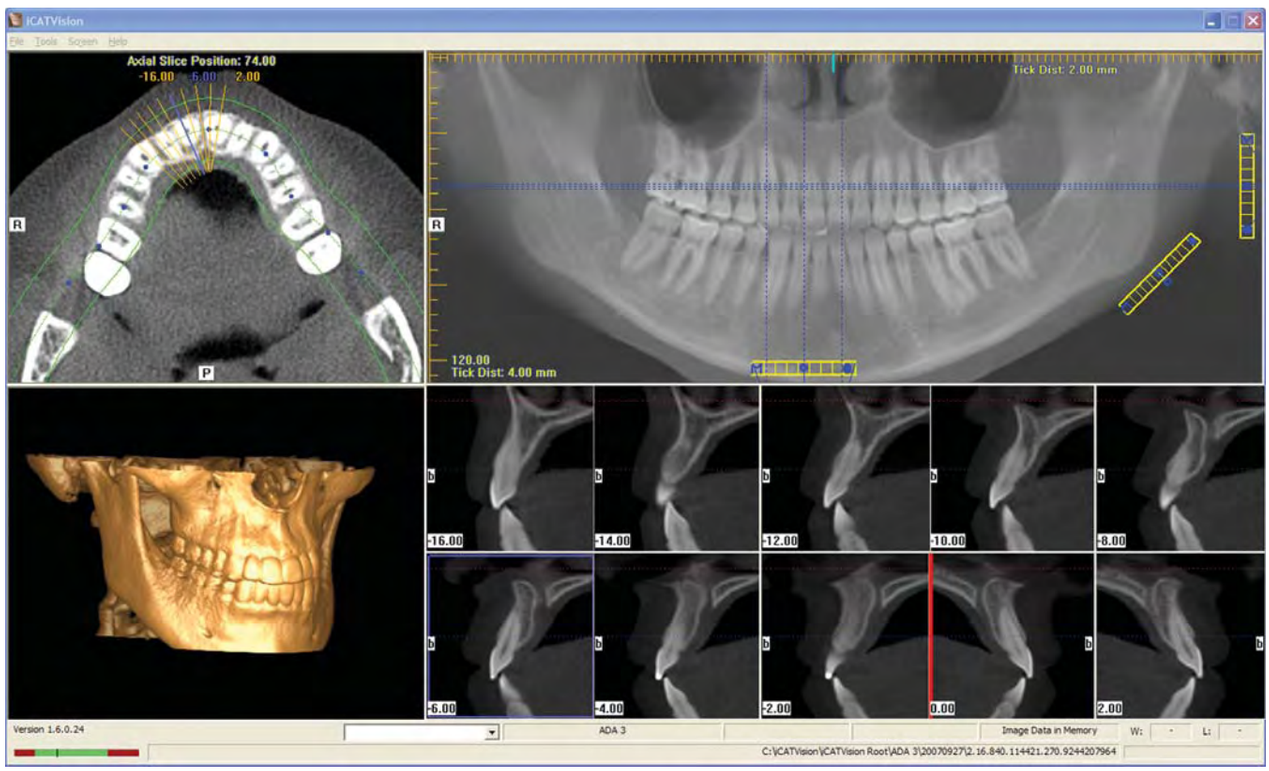

FIGURE 8-1. Cone beam computed tomography (CBCT) data display four primary views: the axial view **(A),** the panoramic view **(B),** the three-dimensional reconstructed view **(C),** and the cross-sectional views **(D).**

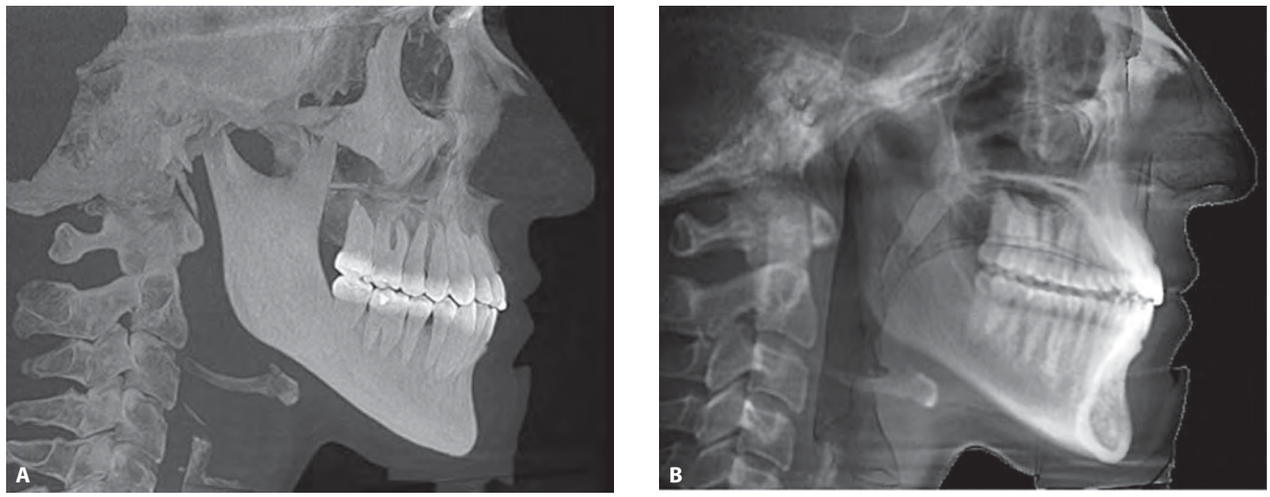

FIGURE 8-2. **A** and **B,** Large field of view (FOV) machines allow for inspection of the entire maxillofacial complex, which can be displayed in a variety of different formats for diagnostic accuracy.

CASE ONE: CBCT Diagnostics for a Horizontally Impacted Maxillary Canine and More . . .

A 10-year-old boy was referred for a three-dimensional CBCT scan by his orthodontist when it was determined that he had an overretained deciduous canine and a horizontally impacted permanent canine. Two-dimensional radiographs were not sufficient to diagnose the spatial position of the canine relative to adjacent vital structures. With the parent's approval, a scan was performed and the three-dimensional data were reviewed. The mixed dentition can be clearly visualized in the initial view of the maxilla (see Figure 8-4). The horizontally impacted canine can be seen in the upper right side of the image, with confirmation that the contralateral canine had erupted properly.

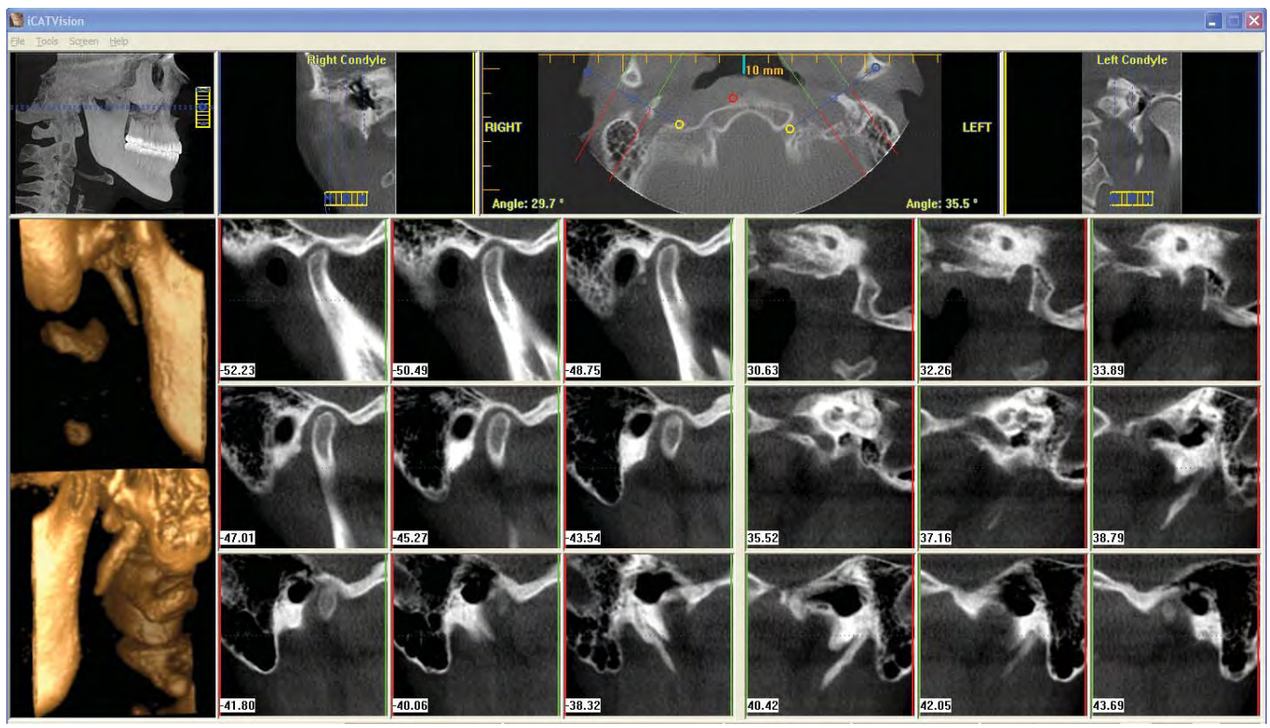

FIGURE 8-3. An example of the diversity displays can be found in the temporomandibular joint (TMJ) view, which automatically creates a series of interactive images focusing on the anatomic landmarks for both the left and the right condyles.

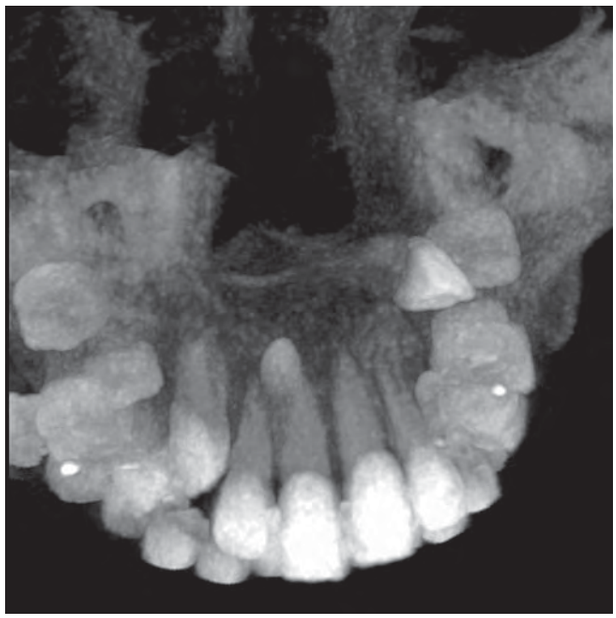

FIGURE 8-4. CBCT scan of mixed dentition in a 10-year-old boy with a horizontally impacted canine tooth.

FIGURE 8-6. The axial view allows inspection of the impacted tooth, the root apex, and proximity to other vital structures including the floor of the nose and maxillary sinus.

Utilizing the CBCT scan data, the maxillary arch was reconstructed as a solid interactive three-dimensional model. The three-dimensional reconstruction accurately revealed the maxillary bone, the properly erupted right canine, the left deciduous canine, and the left impacted canine (see Figure 8-5A). The lateral three-dimensional view exhibited the horizontal position of the permanent canine and the vertical position of the primary canine (see Figure 8-5B). Proximity to adjacent vital structures can also be appreciated in this view. However, the author recommends that all views be assimilated before a definitive diagnosis and treatment plan is determined. The axial view allows further inspection of the

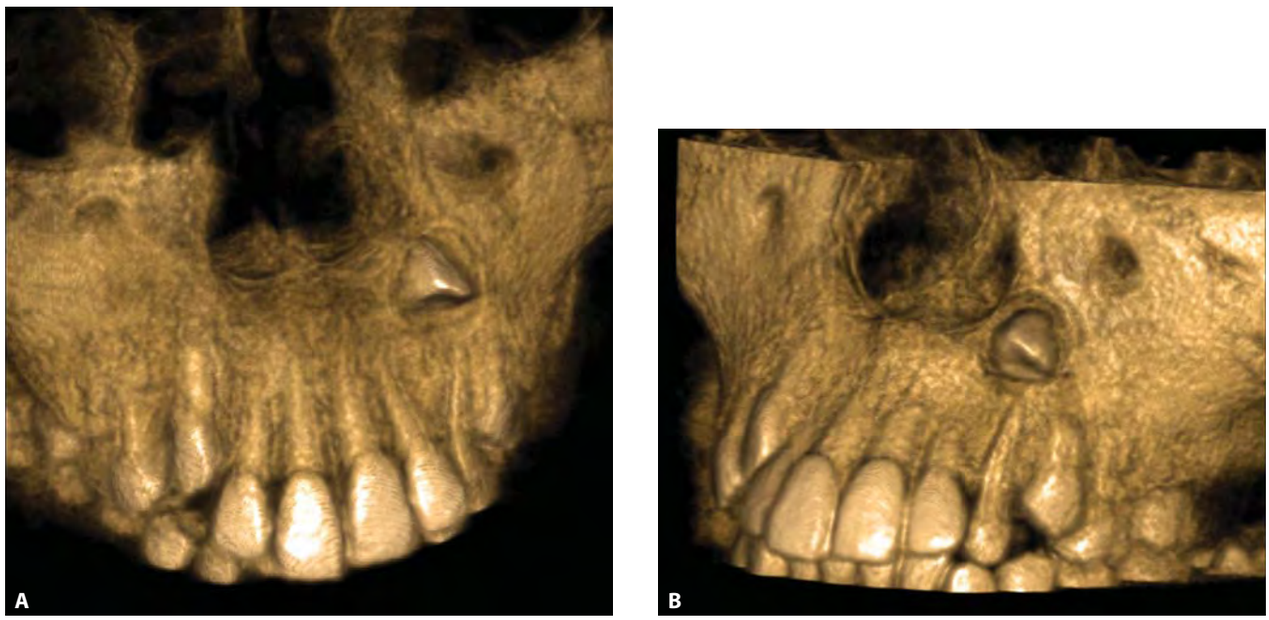

FIGURE 8-5. **A,** Three-dimensional reconstruction reveals the right canine, left deciduous canine, and left impacted canine. B, The lateral view reveals the horizontal position of the impacted canine and vertical position of the primary canine.

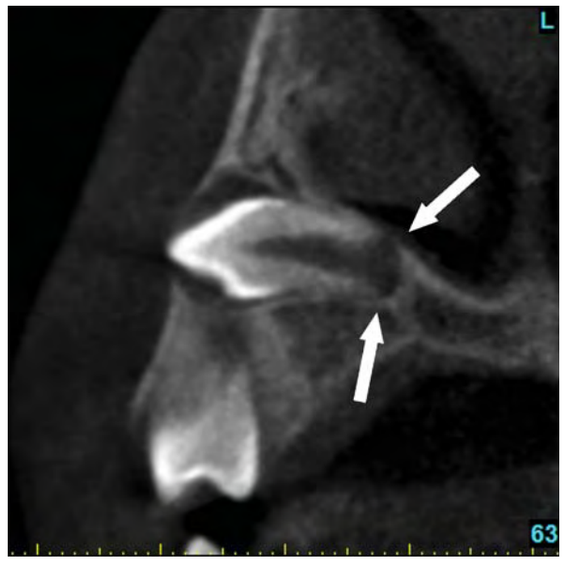

FIGURE 8-7. The cross-sectional view revealed the lack of closure of the root apex, and surrounding structures.

impacted tooth and root apex (see Figure 8-6). The root apex was not fully developed, a fact to be considered if it was determined that the canine tooth could be orthodontically moved into a proper position. The axial view also displayed adjacent vital structures such as the floor of the nose and the maxillary sinus (see *arrows*). Confirmation of the location of the tooth and its proximity to vital anatomy was found in the cross-sectional slice (Figure 8-7). The status of the root apex was also confirmed (see *arrows*).

Using the maximum-intensity projection (MIP), one method of mapping three-dimensional points to a two-dimensional plane, the mixed dentition was clearly visualized but was difficult to interpret, which can sometimes lead to an unexpected incidental finding (Figure 8-8A). Further inspection of the three-dimensional data revealed a supernumerary tooth (mesiodens) near the right maxillary central incisor (see Figure 8-8B). The axial image (Figure 8-9) confirmed the palatal position *(yellow arrow)* and close proximity to the incisal canal *(white arrow)*. A series of cross-sectional image slices (44–49) revealed the 180-degree vertically rotated position of the second impacted tooth and radiolucent area surrounding the clinical crown (Figure 8-10).

The valuable information acquired through three-dimensional imaging technology was essential in accurately diagnosing two impacted teeth within the maxillary scan. Once this information was assimilated, a proper plan of treatment was developed and discussed by all members of the treatment team: the oral surgeon, the orthodontist, and the prosthodontist. The three-dimensional images allowed for improved communication between members of the team, providing the necessary information for a proper course of treatment resulting in a successful outcome.

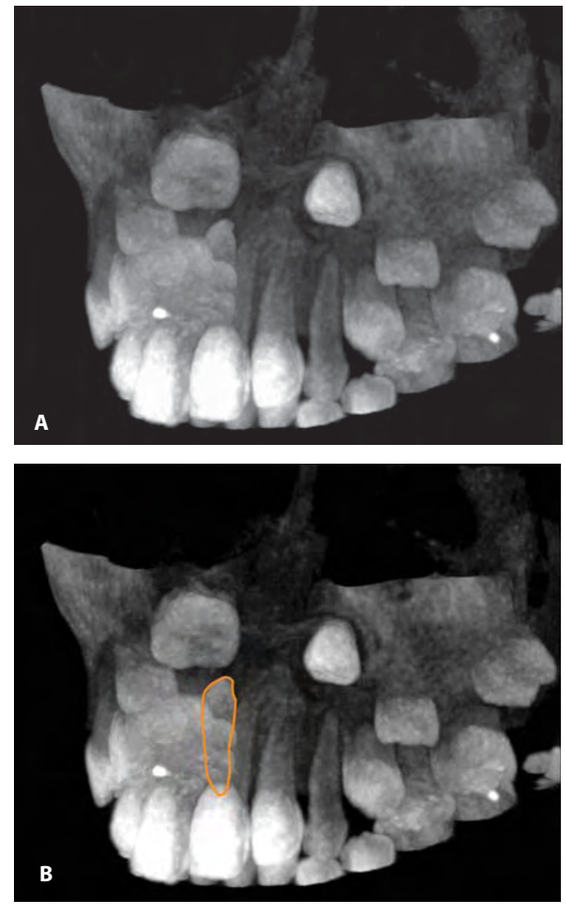

FIGURE 8-8. **A,** Another view of the mixed dentition was helpful to identify other important structures which might have been missed. **B,** A second impacted tooth was found on further inspection of the 3-D images.

FIGURE 8-9. The axial reveals a mesiodens located palataly to the right central incisor tooth (yellow arrow) with close proximity to the incisal canal (white arrow).

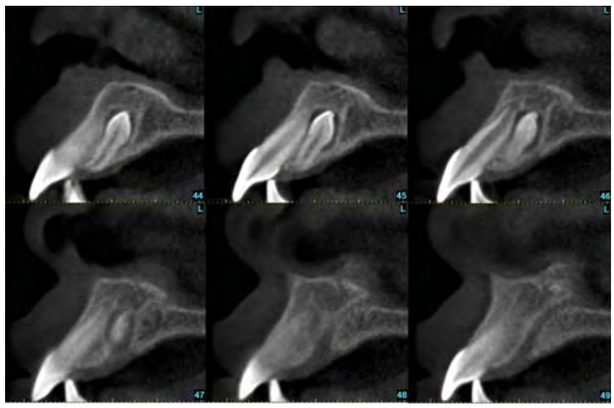

FIGURE 8-10. The cross-sectional slices (44-49 clearly illustrate the position and shape of the mesiodens and radiolucent area surrounding the clinical crown.

CASE TWO: CBCT Diagnostics for a Mandibular Implant Evaluation and More . . .

A 60-year old-man requested an evaluation and treatment recommendation for two missing mandibular first molar teeth. Clinical examination was unremarkable except for the volumetric change in the bone as a consequence of tooth loss. His chief complaint was that he wanted to restore the spaces in his lower arch; he had no other symptoms. A periapical radiograph revealed a suspicious radiolucent area anterior to the potential implant receptor site (see Figure 8-11A). The *arrows* indicate the outline of the area. The intraoral view showed that the mandibular right lateral incisor, canine, and two bicuspid teeth were all within normal limits (see Figure 8-11B). Due to the loss of bone in the first molar area, the proximity to the inferior alveolar nerve, and an irregular appearance on the two-dimensional radiograph, a CBCT scan was recommended.

FIGURE 8-12. Panoramic reconstructed view reveals a well-defined mandibular right lesion.

The panoramic reconstructed view from the CBCT data revealed the potential implant receptor sites in the areas of the mandibular first molar teeth. An unexpected incidental finding further reinforced the need for three-dimensional assessment of patient anatomy. A well-circumscribed lesion was detected in the areas of the mandibular canine and premolar teeth (see Figure 8-12). Further inspection of the cross-sectional images revealed the size and extent of the lesion within the mandible and in relation to the adjacent teeth (see Figure 8-13). The lesion was radiolucent within the confines of the dense facial and lingual mandibular cortical plates (see Figure 8-14). The lesion was accurately measured in all dimensions. The three-dimensional reconstructed image showed the area of the missing right mandibular molar and its proximity to the mental foramen (see Figure 8-15).

The axial slices illustrated the well-circumscribed lesion from a different view, revealing a solid anterior border within the symphysis (see Figure 8-16). The path of the inferior alveolar nerves had been previously traced in *orange.* The scope of the lesion seemed to extend to the right mental

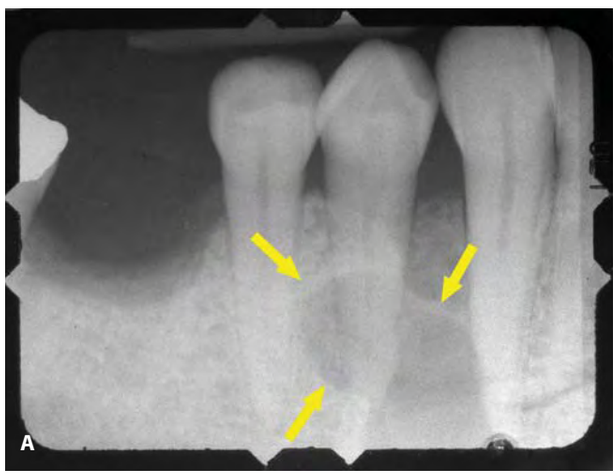

FIGURE 8-11. **A,** A periapical radiograph revealed a suspicious radiolucent area. **B,** Intraoral view.

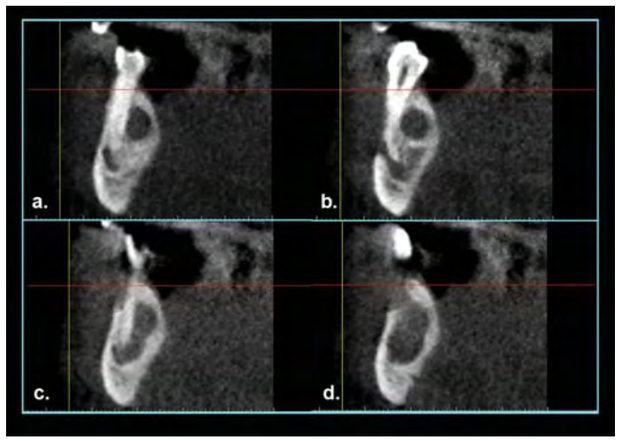

FIGURE 8-13. Cross-sectional images reveal the extent of the lesion within the mandible and in relation to the adjacent teeth.

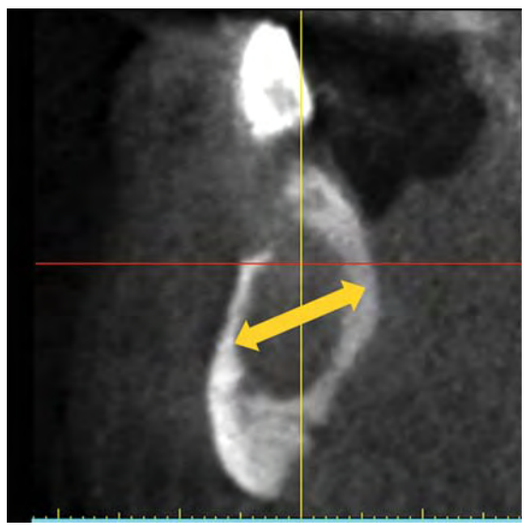

FIGURE 8-14. The radiolucent lesion and the buccal and lingual cortical plates can be visualized and measured *(arrow)* in all dimensions.

FIGURE 8-15. Native three-dimensional reconstructed view of the right side mandible with a missing first molar tooth.

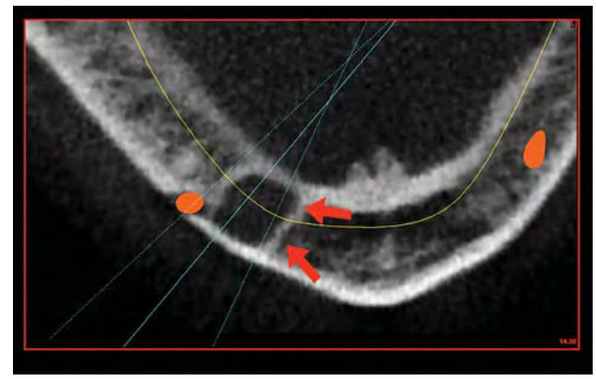

FIGURE 8-16. The axial view reveals a well-circumscribed lesion *(arrows)* near the mental nerve.

foramen as seen in the axial view (see Figure 8-17A). To determine whether the lesion was expansive, accurate measurements were made from the facial to the lingual cortical plates over the lesion and in the area of the contralateral side of the mandible (see Figure 8-17B). The

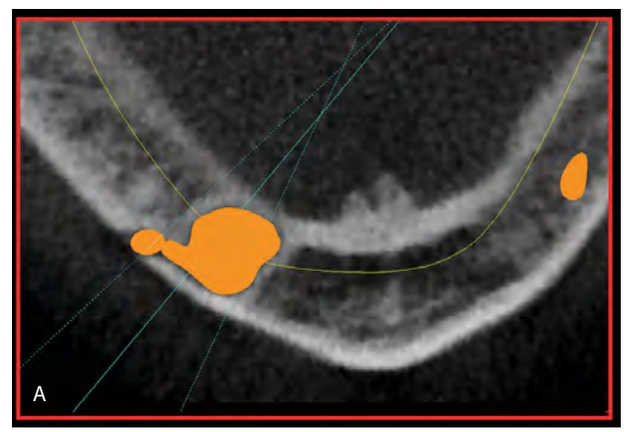

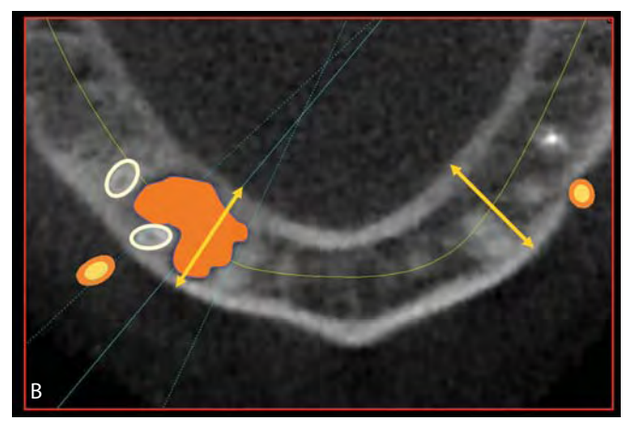

FIGURE 8-17. **A,** The extent of the lesion is marked in *orange.* It appears to extend to the right mental foramen. **B,** Measurements of the right and left side areas indicate that the lesion is nonexpansive in nature.

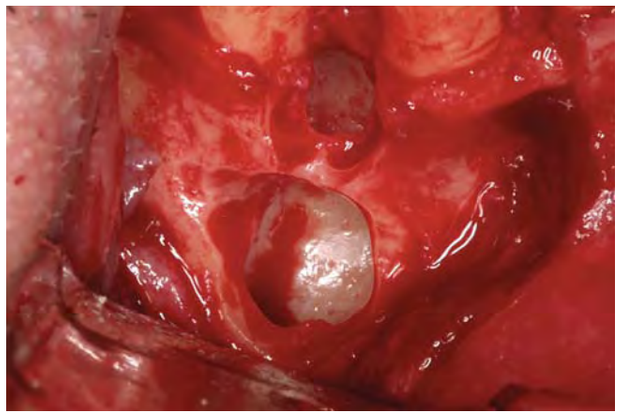

FIGURE 8-18. After excision of the lesion, the shiny lingual cortical plate can be seen. Photo Courtesy of Dr. Richard Kraut

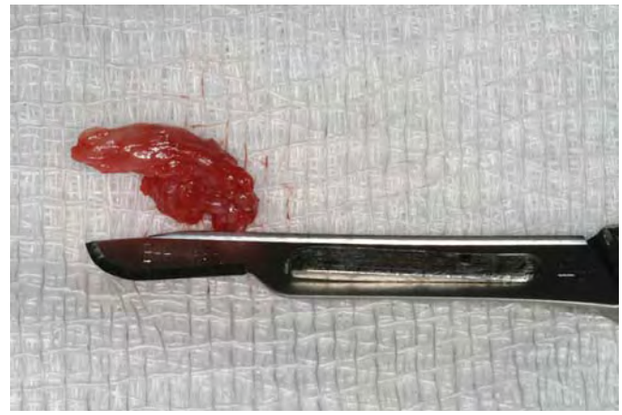

FIGURE 8-20. Part of the excised lesion, sized near the scalpel, was sent for biopsy. Photo Courtesy of Dr. Richard Kraut

measurements were the same, indicating a nonexpansive lesion. Due to proximity to the adjacent teeth, pulp tests were performed and both teeth were found to be vital. The patient was advised of the findings and referred to an oral surgeon. The nature of digital data workflow and CBCT data provides clinicians with one of the best communication tools for diagnosis and treatment planning. The data set was sent via email to the local surgeon for review and discussion. The surgeon was able to view the interactive data and offer a plan for treatment after consultation with the referring dentist. The information was reviewed with the patient and, based upon a thorough review of the findings, it was agreed that a surgical intervention was recommended.

After local anesthesia was administered utilizing a full-thickness mucoperiosteal flap, the area was exposed, and the lesion was excised leaving a shiny appearance to the lingual cortical plate (Figure 8-18). It was elected to fill the lesion with a sterile, biocompatible natural porous bovine bone mineral matrix (Figure 8-19). The excised lesion was sent for biopsy (Figure 8-20), and the area healed uneventfully. The histologic evaluation indicated that the lesion was an odontogenic keratocyst. This type of lesion has a high recurrence rate, which means that it should be followed carefully after initial treatment. The low dosage of CBCT makes it an ideal modality for postoperative follow-up. The 5-month postoperative CBCT cross-sectional image reveals complete fill of the defect site (Figure 8-21). The postoperative axial view and the resultant density of the grafted site can been seen at 5 months in Figure 8-22. The lesion has been followed for over 3 years without any sign of recurrence (Figure 8-23).

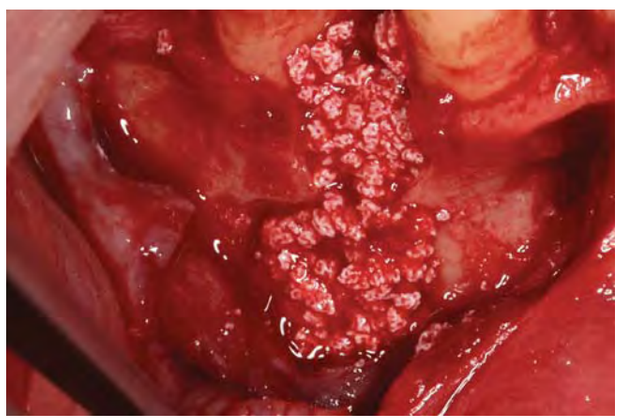

FIGURE 8-19. The lesion was filled with graft material and allowed to heal. Photo Courtesy of Dr. Richard Kraut

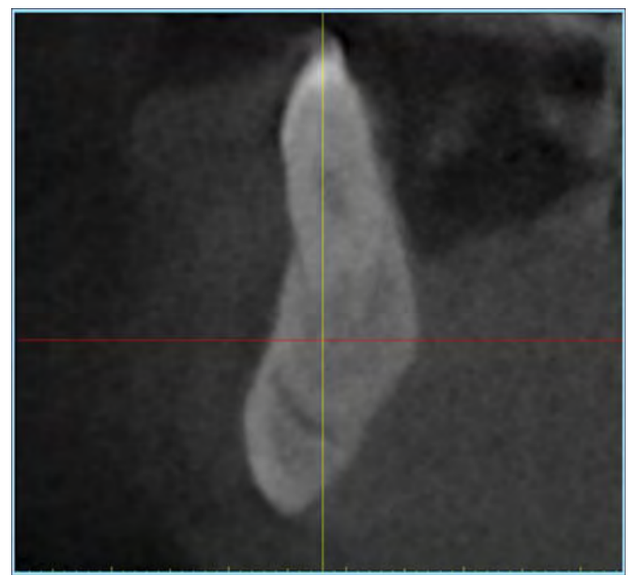

FIGURE 8-21. The 5-month CBCT postoperative cross-sectional image reveals complete fill of the defect site.

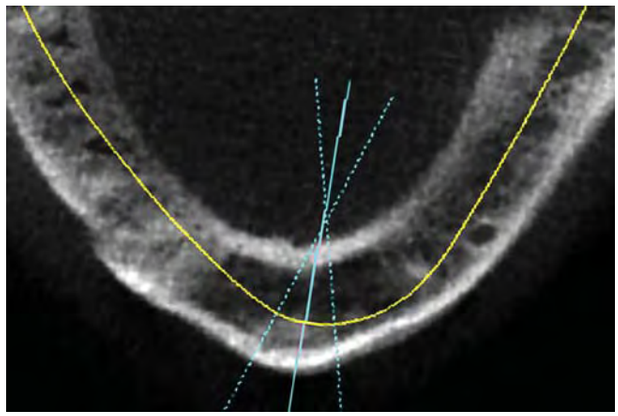

FIGURE 8-22. The postoperative axial view and the resulting density of the grafted site at 5 months.

This case represented a CBCT scan that resulted in an incidental finding of an intra-osseous lesion. Due to the location of the lesion and its proximity to the mental nerve and adjacent teeth, the subsequent treatment could have been debilitating to the patient. The diagnostic accuracy afforded by the three dimensional views allowed for a complete understanding of the size and scope of the lesion, so that the oral surgeon could make an educated decision on the recommended course of treatment. Therefore, the ability to visualize the lesion and its properties are essential for successful outcomes.

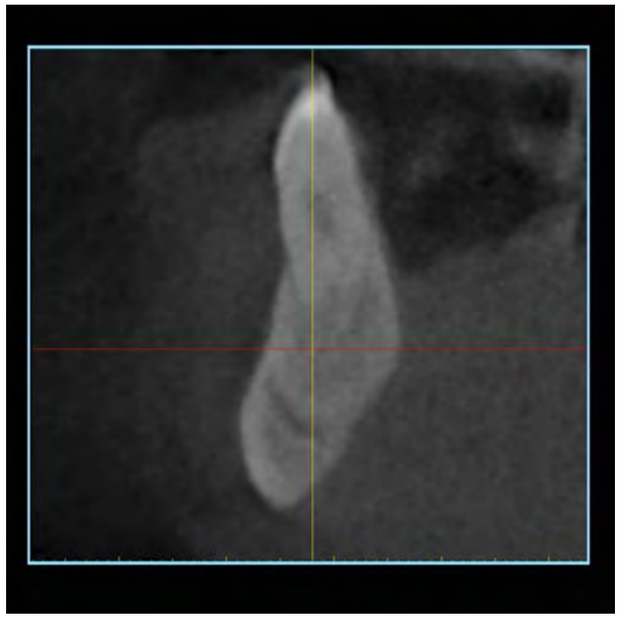

FIGURE 8-23. The CBCT cross-sectional image at the 3-year recall. No evidence of recurrence.

CASE THREE: CBCT Diagnostics to Assess Potential Graft Augmentation

A 17-year-old female was referred for routine dental implant evaluation of a congenitally missing maxillary left lateral incisor. Clinical examination revealed a facial concavity in the area of the missing tooth, leaving a narrow facial-palatal dimension of bone for an implant. Conventional periapical radiographs were not helpful in determining the quality of the bone, the width of bone, or the thickness of the facial or palatal cortical plates. Further radiographic studies were suggested and a CBCT scan was performed.

The panoramic reconstructed view based upon the CBCT data revealed blunted root apexes for the maxillary anterior teeth and allowed inspection of the potential lateral incisor implant receptor site (see Figure 8-24). To gain an understanding of the space required to place and restore a single implant in the esthetic zone, all three-dimensional views were considered. The axial view sliced near the crest of the bone displays the root morphology of the entire arch and the facial-palatal width of the residual alveolar crestal bone (see Figure 8-25). The shape of the individual teeth as seen in the axial view demonstrates what the author has termed as the "restorative dilemma". The shape of our natural teeth as they emerge from the bone are consistent with normal tooth morphology. The dental implants we may use to insert into the bone are "round" in shape. Going from the round shape of the implant to a morphologically correct tooth form is not easy. It is a restorative dilemma.

Utilizing nondistorted measuring tools in the axial view *(red),* the facial-palatal dimension can be determined for the right existing lateral incisor tooth, as transposed to the left lateral space (see Figure 8-26). A realistic implant known to be 3.8 mm in diameter can be virtually placed to assess the potential volumetric space requirements of this receptor site *(yellow arrow).* The narrow ridge can then be assessed in the cross-sectional views (see Figure 8-27A). Utilizing specialized three-dimensional planning software, a simulated bone graft can be positioned on the facial aspect of the alveolar ridge (see Figure 8-27B). If this were to be a block graft taken from mandibular ramus or the anterior symphysis fixation would be an issue to ensure success—and this aspect can also be virtually planned (see Figure 8-28B and C). The

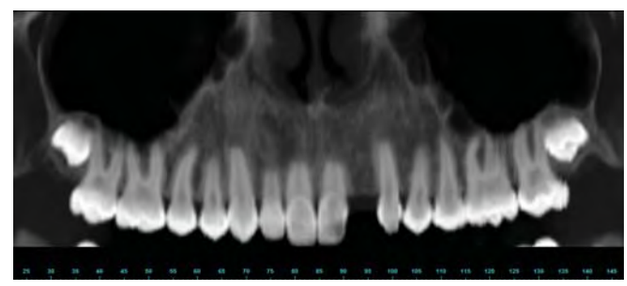

FIGURE 8-24. Panoramic reconstructed view reveals a congenitally missing maxillary left lateral incisor.

FIGURE 8-25. Axial view shows the facial-lingual dimension of the left lateral incisor area.

length and diameter of the fixation screw should be commensurate with the graft thickness and density of the underlying host bone. Once an appropriate ridge width and volume has been achieved, the implant can be planned.

In research developed in 1992 and first published in 1995, the author proposed a method for receptor-site evaluation within the cross-sectional slice depicting the available bone. This concept is called the *Triangle of Bone® (TOB)*. The base of the triangle is created by drawing a line from the widest portion of the facial bone to the widest portion of the palatal bone. The apex of the triangle is positioned above the alveolar crestal bone (or proposed position of the crest when considering grafting), and the lines are connected. The most ideal position to maximize bone volume surrounding an implant would be to bisect the triangle. A realistic 3.8-mm-diameter tapered-design implant placed within the TOB is surrounded by bone in the apical two thirds, leaving the

FIGURE 8-26. The axial view allows for precise measurements (in *red*) to compare the right side existing lateral incisor with the potential space requirements for the implant receptor site *(arrow)*.

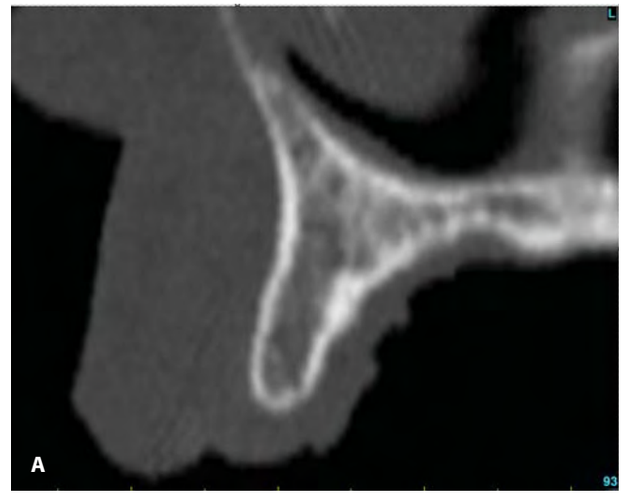

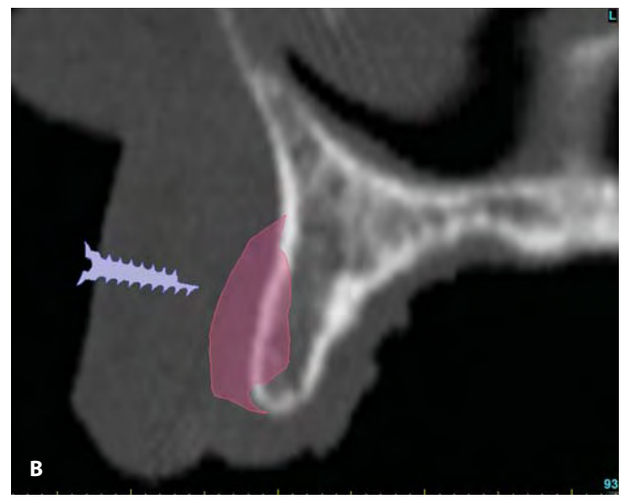

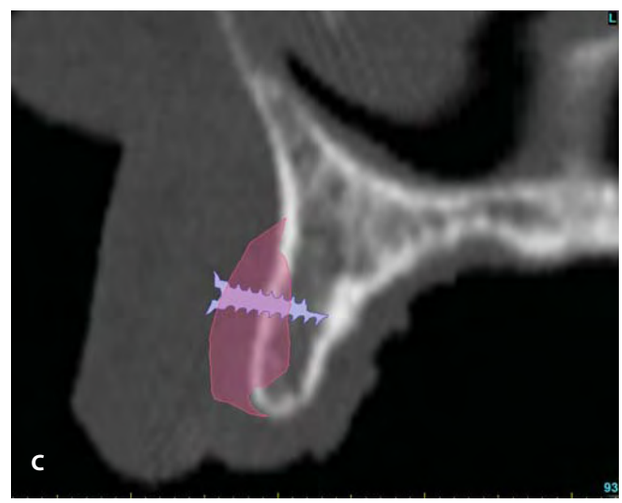

FIGURE 8-27. The cross-sectional view shows a narrow ridge **(A),** a simulated bone graft **(B),** and the plan for fixating the donor graft with a screw **(C).**

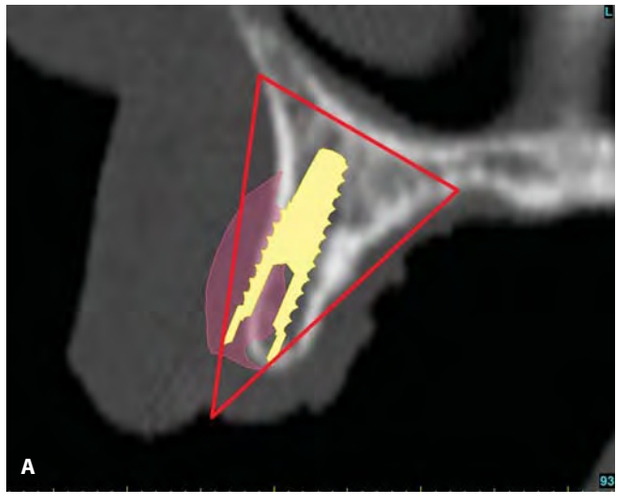

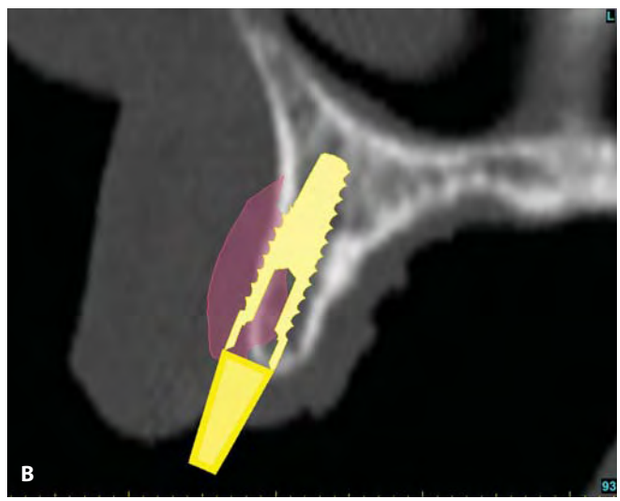

FIGURE 8-28. A simulated 3.8-mm diameter implant positioned within the "triangle of bone" **(A)** and a simulated abutment to help visualize the emergence profile **(B).**

facial aspect exposed to the simulated bone graft (see Figure 8-29A). However, the goal of implant dentistry is not the implant, it is the tooth. Therefore, the restorative aspect must be considered before finalizing the placement of the implant. The abutment simulation helps to visualize the path of emergence of the implant within the envelope of the restoration (see Figure 8-29B).

The three-dimensional planning concepts and software tools have empowered clinicians with new paradigms for assessing implant and/or grafting sites. Closer inspection of the positioning of the simulated bone graft, implant, abutment, and virtual tooth reveals that at the facial-coronal aspect of the implant, there is 1.65 mm of new simulated bone, 2.93 mm at the middle of the implant, and 1.65 mm on the palatal aspect near the first thread (see Figure 8-30). A virtual tooth has been properly positioned within the space requirements for a left lateral incisor tooth. A 12-degree angulated abutment has been simulated to fall within the envelope of the virtual tooth for

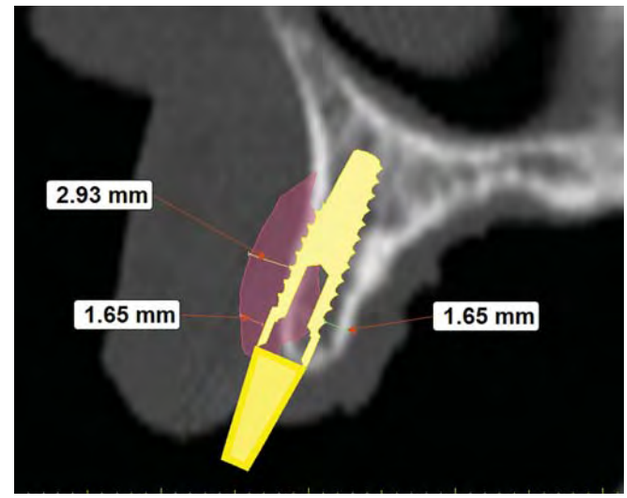

FIGURE 8-29. Closer inspection of the positioning of the simulated bone graft, implant, abutment, and virtual tooth reveals that at the facial-coronal aspect of the implant, there is 1.65 mm of new simulated bone, 2.93 mm at the middle of the implant, and 1.65 mm on the palatal aspect near the first thread.

assessment of emergence profile for the planned cemented-type restoration. However, final verification of bone graft and implant placement should be completed utilizing the three-dimensional reconstructed model.

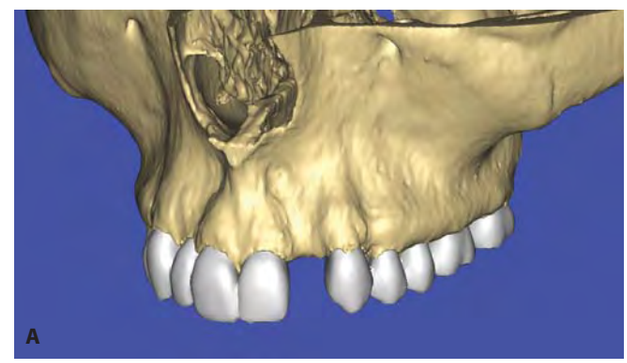

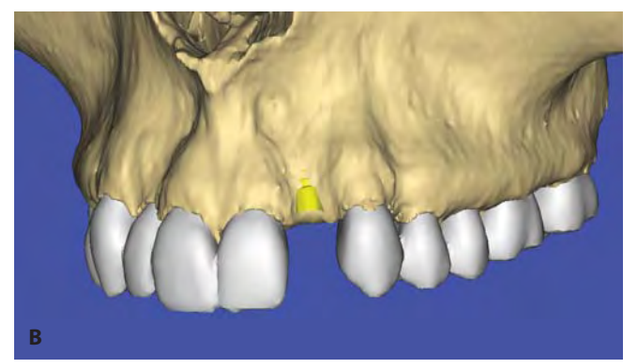

FIGURE 8-30. The three-dimensional reconstruction reveals the severe concavity of the lateral incisor area **(A),** with a simulated implant with the coronal aspect exposed at the alveolar crest **(B).**

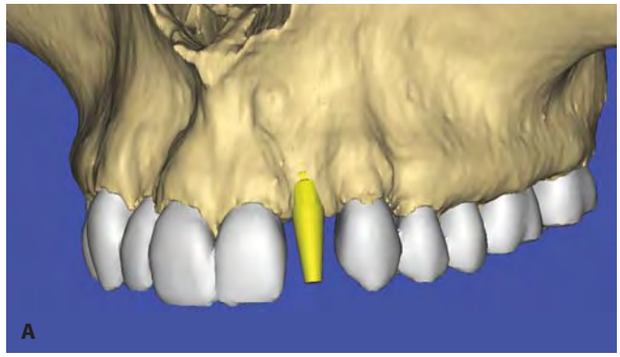

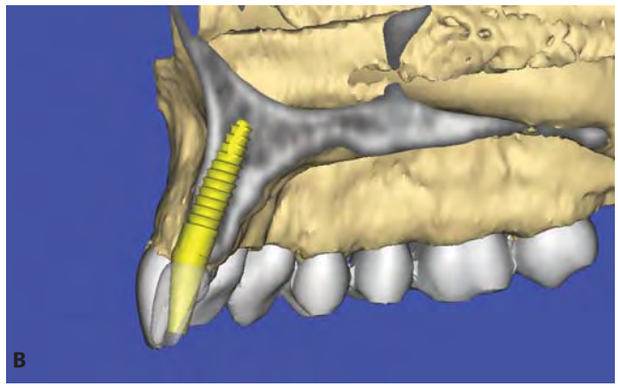

FIGURE 8-31. The abutment projection extends from the implant indicating direction **(A),** which is further demonstrated in the three-dimensional cross-sectional slice through the virtual tooth **(B).**

Examination of the three-dimensional reconstructed maxilla reveals the dentition, the surrounding root eminences, and the resulting concavity in the area of the congenitally missing left lateral incisor tooth (see Figure 8-31A). The placement of a simulated implant helps to visualize the depth of the concavity and assess the facial exposure of the coronal aspect of the implant (see Figure 8-31B). An abutment projection that extends from the implant is helpful in determining implant positioning and angulation (see Figure 8-32A).

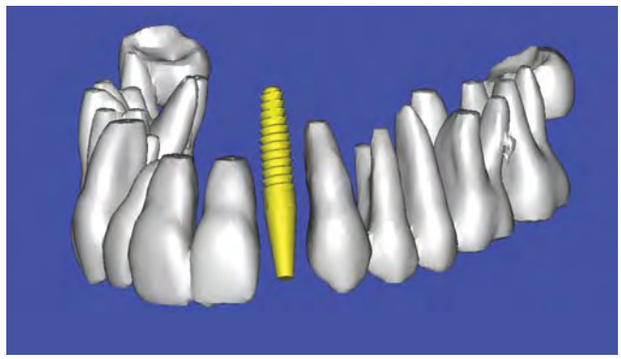

FIGURE 8-32. Removing the bone allows access to the root morphology of the adjacent teeth.

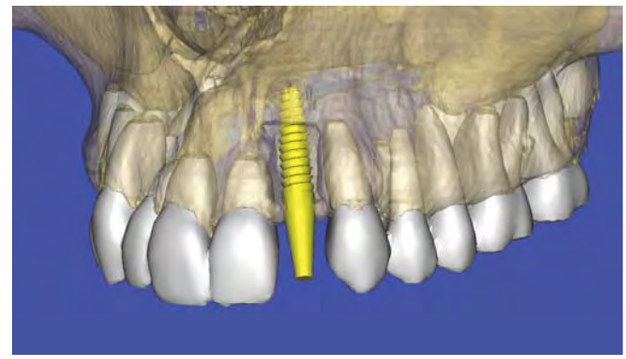

FIGURE 8-33. Using "selective transparency" reveals the implant and abutment projection within the planned receptor site.

Using advanced "clipping" features of the planning software, the three-dimensional maxilla can be sliced to provide additional vital information regarding the implant position and abutment within the envelope of the virtual tooth (see Figure 8-32B). The proximity of the implant to the adjacent teeth can be confirmed by removing the maxillary bone and leaving only the clinical crowns and tooth roots (see Figure 8-32). Interactive treatment planning software can provide a variety of methods to reveal the three-dimensional data, and perhaps, the most striking is the ability to selectively control the opacity of different anatomy, a concept that the author has termed *selective transparency.* Using selective transparency, the outer maxillary bone remains translucent, showing the underlying implant and adjacent teeth and roots (see Figure 8-33).

For illustrative purposes, the bone graft site can be virtually prepared to receive a block bone graft as demonstrated utilizing innovative software modules (Figure 8-34A). The facial bone has been modified, and the simulated receptor site de-corticated for better vascularity to the graft (see Figure 8-34B). Using the a special "graft volume tool" the prepared defect site can be virtually filled with an adequate volume of bone to support an implant based upon the paradigms addressed previously (see Figure 8-35). The fixation of the graft can also be visualized in advance of the procedure for proper positioning within the graft and the receptor site bone (see Figure 8-36A and B). Through three-dimensional "clipping," the entire surgical and restorative complex can be visualized including the implant, the bone graft, the abutment, and the virtual tooth (Figure 8-37). The final simulation on the three-dimensional reconstructed maxilla is useful as an educational tool to explain the individual process to the patient, and a communication tool to the referring clinician regarding all of the components of the procedure (Figure 8-38). The implant can be seen emerging from the proposed bone graft (see Figure 8-38A), the virtual translucent tooth (see Figure 8-38B), the opaque tooth helpful in evaluating contact area in relation to the interproximal height of bone (see Figure 8-38C), and a simulation of the healed graft site with the restoration in place (see Figure 8-38D). This case highlighted the wide

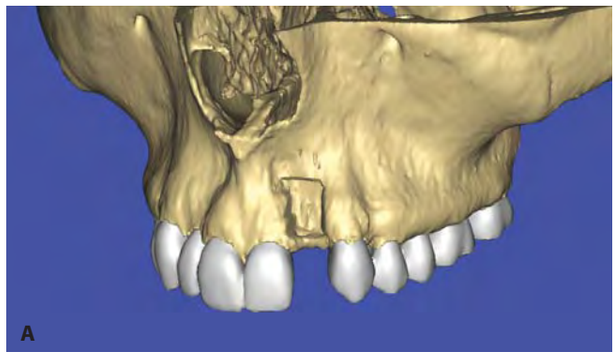

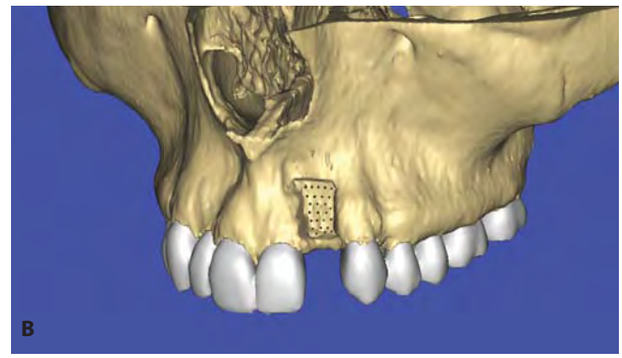

FIGURE 8-34. Using three-dimensional planning tools, the simulated graft receptor site can be virtually "prepared" **(A)** and the bone decorticated **(B).**

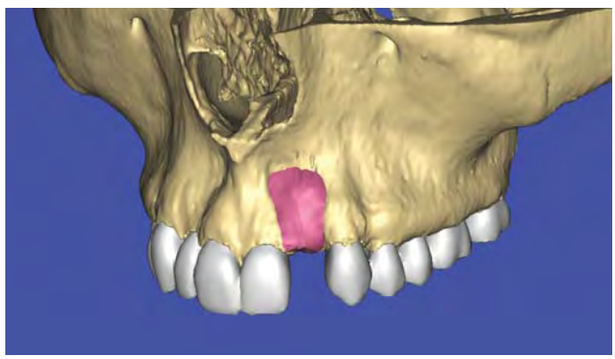

FIGURE 8-35. The graft site can be simulated to fill the concavity to allow for adequate volume of bone to support an implant.

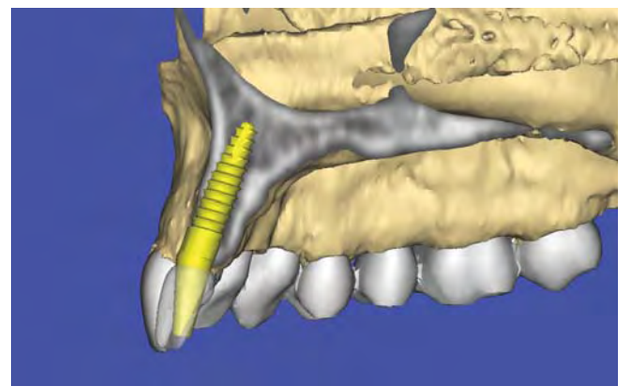

FIGURE 8-37. The implant, the graft, the abutment, and virtual tooth can be visualized.

variety of tools that can be utilized to enhance the diagnostic and treatment capabilities for a single tooth and bone augmentation application.

CASE FOUR: CBCT Diagnostics in the Mandible—Implants and More . . .

A 62-year-old man presented with complete maxillary and mandibular removable dentures. He wished to review treatment options for implant-supported restorations, both fixed and removable. As part of the presurgical prosthetic workup, maxillary and mandibular study casts were fabricated to facilitate capturing vertical dimension records. A complete denture setup was achieved with the appropriate tooth mould to fit the arch form. Although it appeared that the patient had adequate bone for implant placement, in order to plan with greater accuracy, a barium sulfate scanning template was fabricated by duplicating the tooth setup (BariOpaque®, Salvin Dental, Charlotte, NC). The scanning template was placed intraorally, with a putty bite registration to stabilize

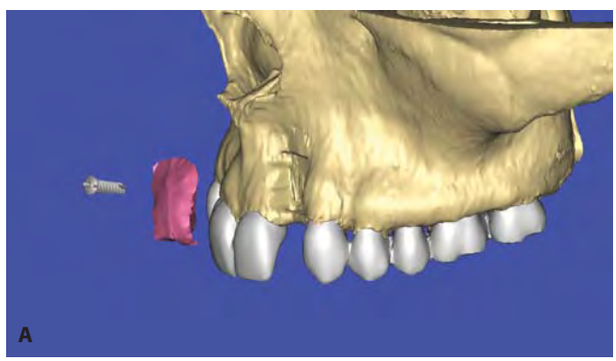

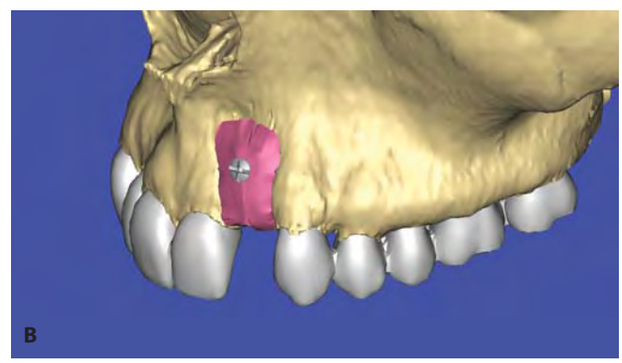

FIGURE 8-36. **A,** The fixation screw can also be visualized for proper positioning within the graft. **B,** The fixation screw in place.

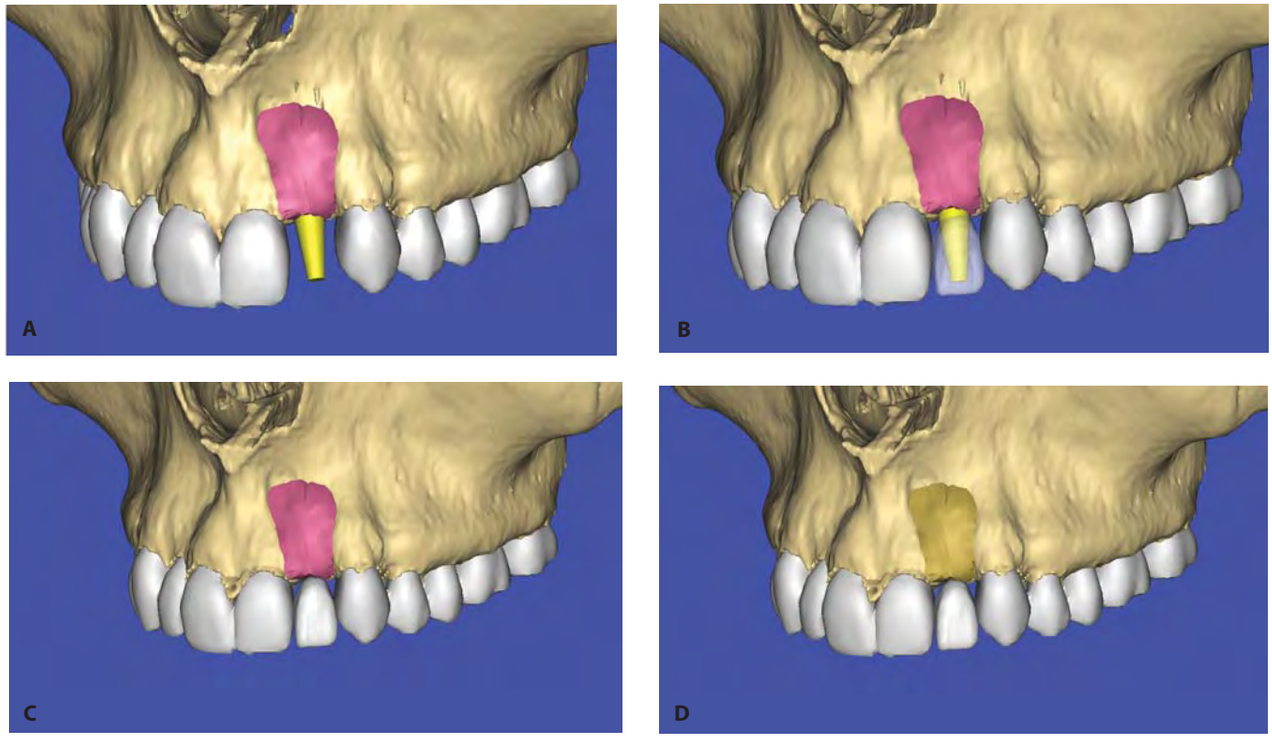

FIGURE 8-38. The implant abutment emerging from the graft **(A),** with the virtual translucent tooth **(B),** the virtual tooth (opaque) **(C),** and a simulation of the healed graft and restoration in place **(D).**

the maxillary and mandibular position and to minimize movement before the CBCT scan. The panoramic radiograph with the mandibular barium sulfate scanning template can be seen in Figure 8-39. For the purposes of this chapter, only the information from the mandible is presented.

The three-dimensional reconstructed view allows for inspection of the mandibular morphology and an appreciation of the mental foramina (see Figure 8-40). However, it does not reflect the relationship between the bone and the desired occlusion. A properly fabricated radiopaque scanographic template affects the treatment plan by linking the tooth position to the underlying bone, establishing important landmarks that help to direct implant positioning (see Figure 8-41 A and B). Whereas it is possible to simulate the placement of implants in the anterior symphysis without a template, there is no assurance that the implants can be restored properly within the boundaries of the restorative envelope (see Figure 8-42). Noting the location of the mental foramen and the path of the inferior alveolar nerve is essential to avoid potential serious complications. Most interactive treatment planning software applications will provide the necessary tools to trace out the nerve from the lingula to the mental foramen. Using the cross-sectional images, the location of the mental foramen can be located and the nerve traced (see Figure 8-43). Once the nerves have been located, the implants can be placed at the desired position within the confines of the scanning template. Ideally, the implant should be positioned within the bone, with an abutment pro-

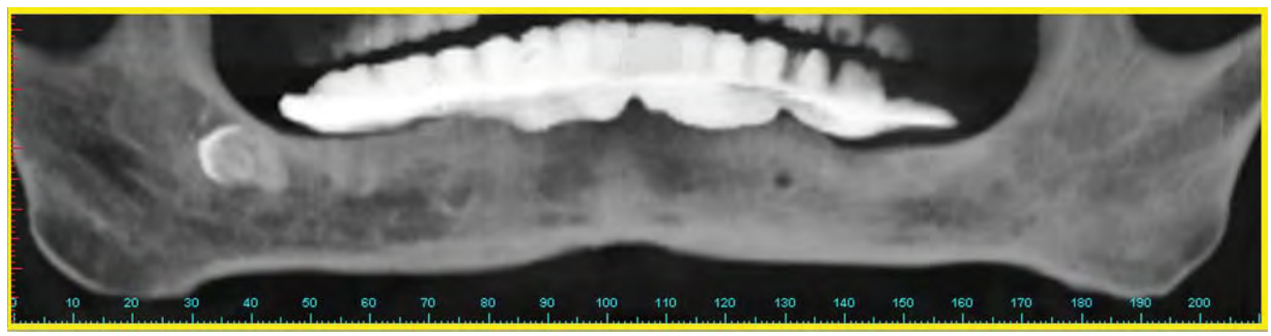

FIGURE 8-39. Panoramic radiograph with mandibular barium sulfate template.

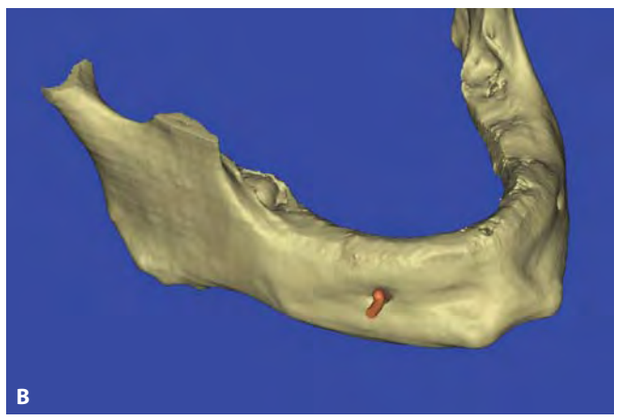

FIGURE 8-40. **A** and **B,** Mandibular reconstructed three-dimensional view shows the simulated nerve at the right mental foramen.

jection extending above the occlusal plane and adjusted after taking into consideration the other views (see Figure 8-44A). Note the difference in bone quality, density, and morphology from one implant receptor site to the next (see Figure 8-44B). Implant length and diameter can also be evaluated in the cross-sectional view.

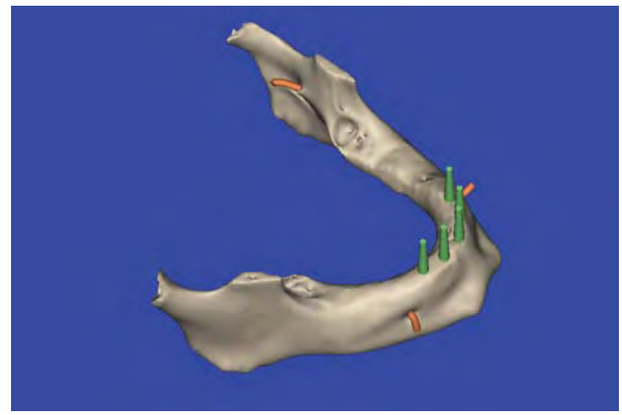

FIGURE 8-42. Five simulated implants placed in the anterior mandible.

Returning to the three-dimensional reconstructed model and the occlusal view, the inter-implant distances and angulation can be evaluated to fit the needs of the restorative scheme. If desired, the software can help to parallel the implants (see Figure 8-45A). Using the concept of selective transparency, the path of the mental nerves and proximity to the implants can be clearly visualized. The initial positioning of the implants can then be verified by superimposition of the scanning template (see Figure 8-46). Adjustments can be accomplished if necessary. The left distal-most implant exits in the embrasure between the left canine and the first bicuspid tooth. If this were to be a screw-retained hybrid-type restoration, the implant could be repositioned to achieve a better location for the screw access hole. Once the implant positions have been verified, the oral surgeon can confer with the referring clinician, and prepare for the surgical intervention. Based upon the accepted virtual plan, a CT-derived bone-borne or soft-tissue borne template could be fabricated - referred to by the author as "template-assisted" surgery. Or the surgeon can place the implants free-hand, using the CT data as provided by the plan to guide the implant placement

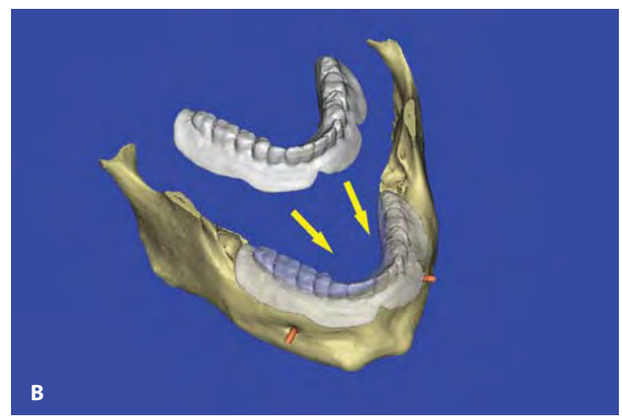

FIGURE 8-41. The radiopaque scanographic template helps visualize desired tooth position in relation to the underlying bone.

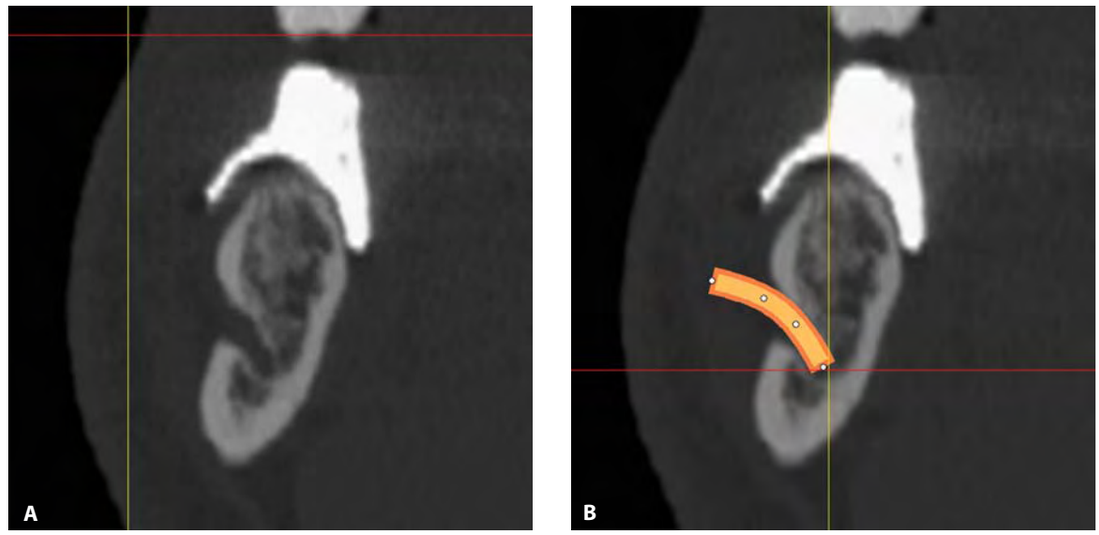

FIGURE 8-43. The mental foramen is noted **(A)** and the path of the mental nerve traced **(B).**

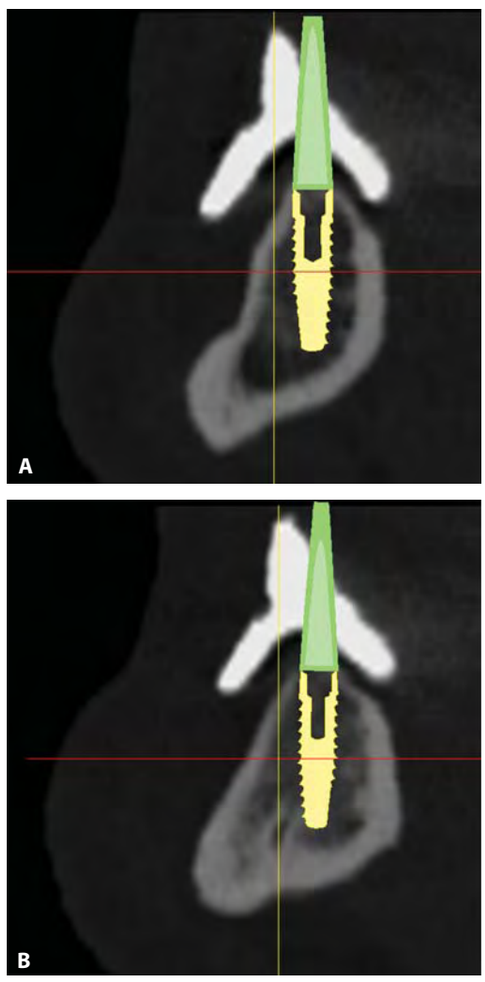

FIGURE 8-44. **A** and **B,** Using the radiopaque template as a guide, implants are positioned within the bone and restorative envelope.

based upon computer print-outs of the various slices - referred to as "CT-assisted" surgery.

Upon inspection of the entire mandible in either the panoramic or axial view, additional significant anatomy

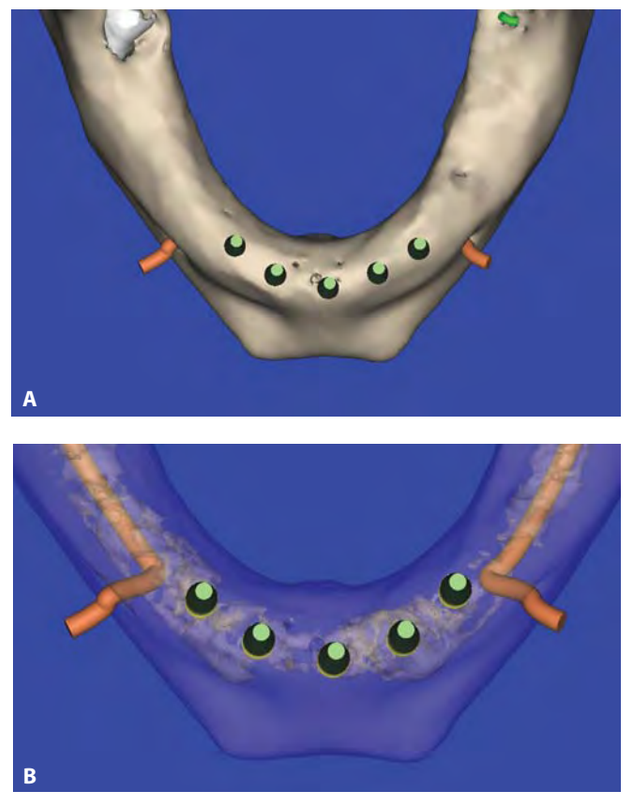

FIGURE 8-45. **A,** If desired, the implants can be placed in a parallel orientation with appropriate implant-to-implant spacing. **B,** Selective transparency allows visualization of the mental nerves and proximity to implant placement.

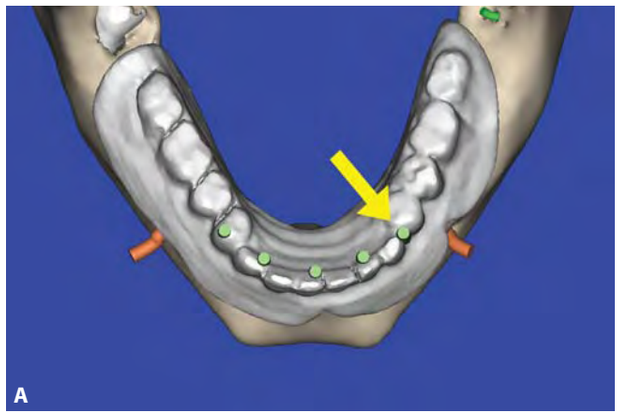

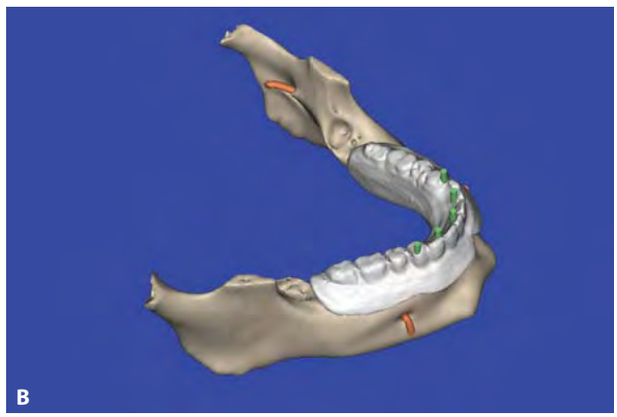

FIGURE 8-46. **A** and **B,** The initial positioning of the implants can be verified by superimposition of the scanning template. The final implant placement can then be finalized based upon the restorative envelope.

was discovered. In the posterior right side mandible, a horizontally impacted molar was identified (see Figure 8-47). The ability to zoom in and focus on a small area of interest is an important feature of three-dimensional imaging technology. The close-up axial view reveals the horizontal tooth position with the clinical crown facing to the lingual (see Figure 8-48A). Scrolling through the next axial slice revealed the dilaceration of roots embedded in the thick facial cortical bone (see Figure 8-48B). The proximity to the inferior alveolar nerve can be confirmed in the cross-sectional view if the nerve had been previously traced to the posterior aspect of the mandible. (see Figure 8-49). If the software allows for the tooth to be virtually separated from the bone, the coronal aspect of the impacted tooth would be visible in the three-dimensional reconstructed view (see Figure 8-50). The area of interest can be expanded to clearly visualize the molar, the extent of the bone surrounding the coronal portion, and its proximity to the path of the inferior alveolar nerve using transparency features of the software (see Figure 8-51). Rotation of the three-dimensional mandible allows for a lingual view of the impacted molar and the relationship to the nerve from another perspective (see Figure 8-52). The bone can be totally removed

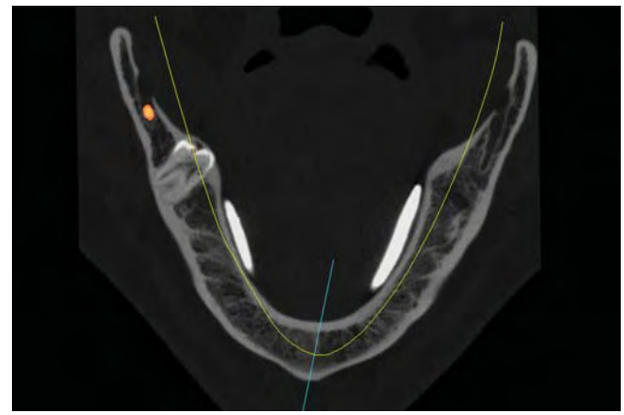

FIGURE 8-47. The axial view revealed a horizontally impacted third molar.

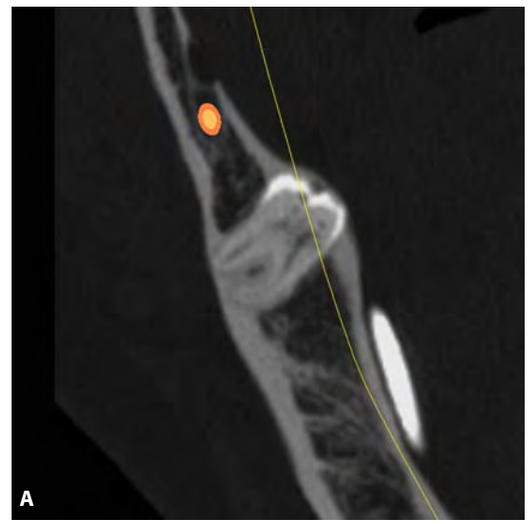

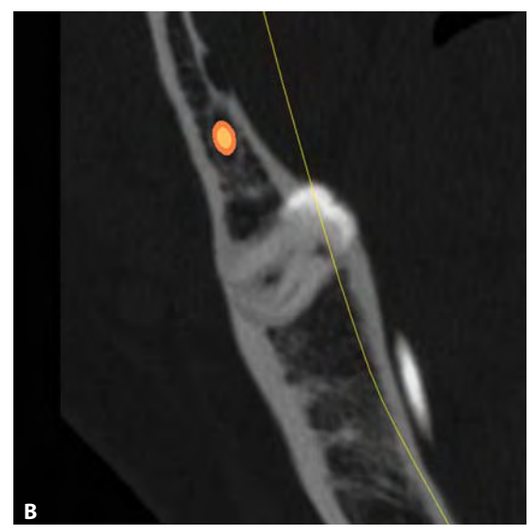

FIGURE 8-48. A close-up axial view reveals the tooth position **(A)** and the dilaceration of the roots embedded in the facial cortical bone **(B).**

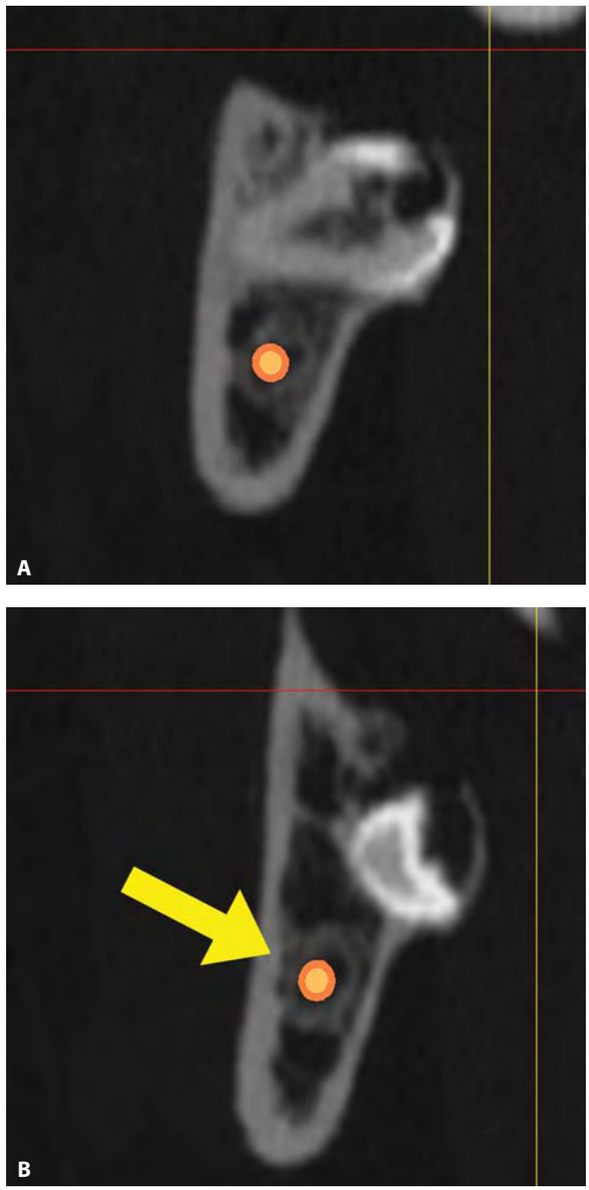

FIGURE 8-49. **A** and **B,** The cross-sectional view illustrates the relationship between the impacted molar and the inferior alveolar nerve.

to provide an even closer inspection of the vital anatomy and root morphology (see Figure 8-53).

Fortunately, in this example, there was adequate spacing between the molar tooth and the nerve to avoid potential damaging complications. If the molar required removal, these views would prove to help guide the oral surgeon in planning the surgical intervention with the least amount of patient morbidity.

If the posterior ramus were to be utilized as a potential donor graft site, the three-dimensional reconstructed view would provide ample information to determine whether the procedure could be successfully accomplished (Figure 8-54).

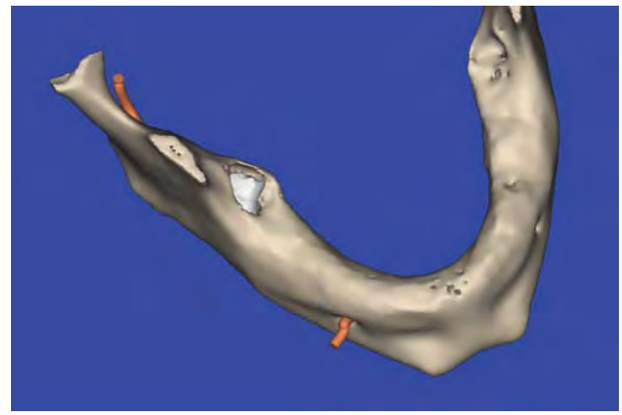

FIGURE 8-50. The three-dimensional reconstructed view reveals the coronal aspect of the impacted molar.

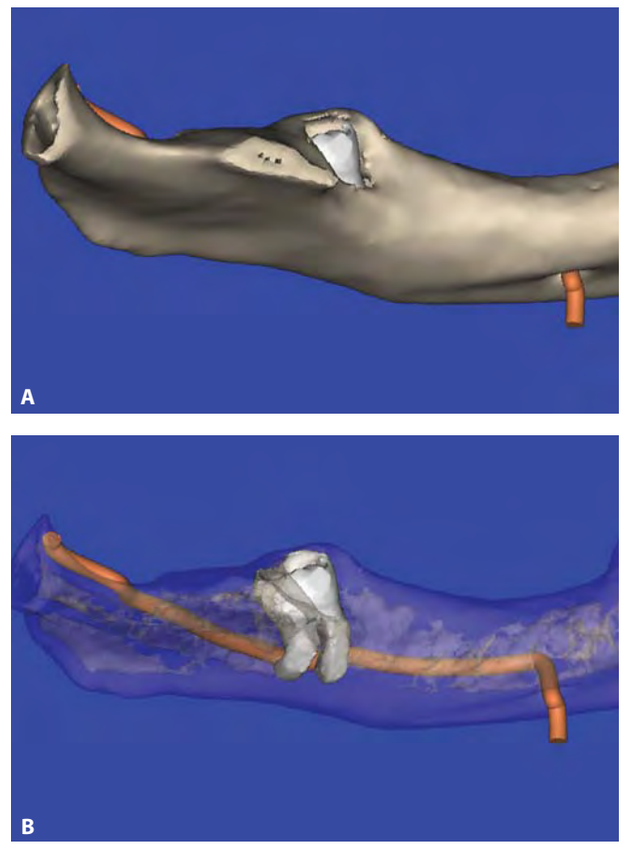

FIGURE 8-51. The close-up view of the impacted molar **(A)** more clearly visualized near the inferior alveolar nerve by modifying the transparency of the mandibular bone **(B)**.

Whereas the bone might look excellent during the harvesting procedure, without a complete understanding of the underlying vital anatomy, complications could occur. Therefore, it is imperative to locate the path of the inferior alveolar nerve in relation to the donor site. The cross-sectional view reveals the thickness of the facial cortical plate and the proximity of

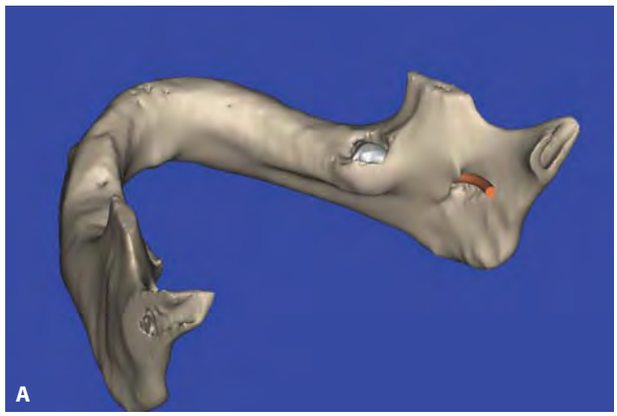

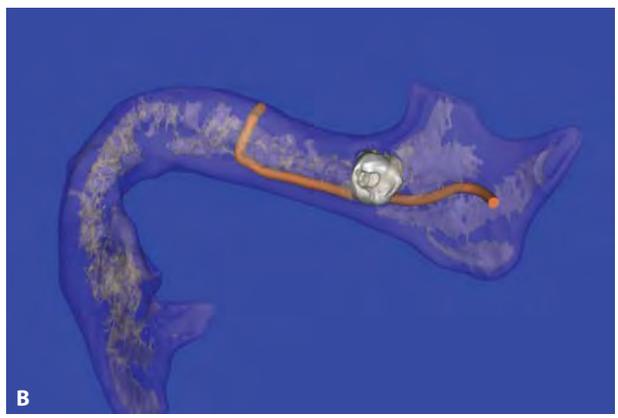

FIGURE 8-52. Rotating the three-dimensional mandible allows for a lingual view of the impacted molar **(A)** and proximity to the inferior alveolar nerve **(B).**

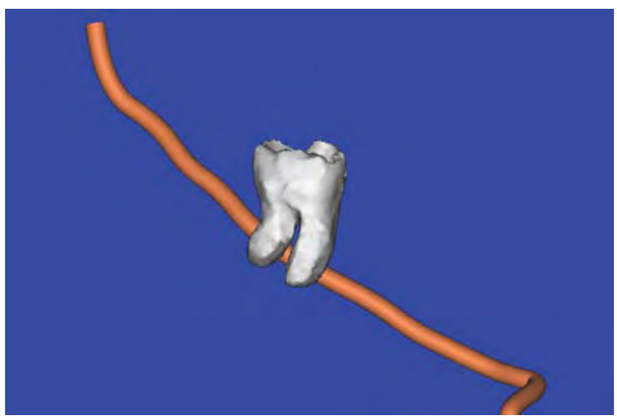

FIGURE 8-53. The bone can be removed totally to allow for a close inspection of the vital anatomy.

the inferior alveolar nerve (Figure 8-55). If there was adequate clearance, and the quality of bone sufficient for the bone to be utilized as a donor, a plan can be formulated that would allow for proper harvesting while limiting potential

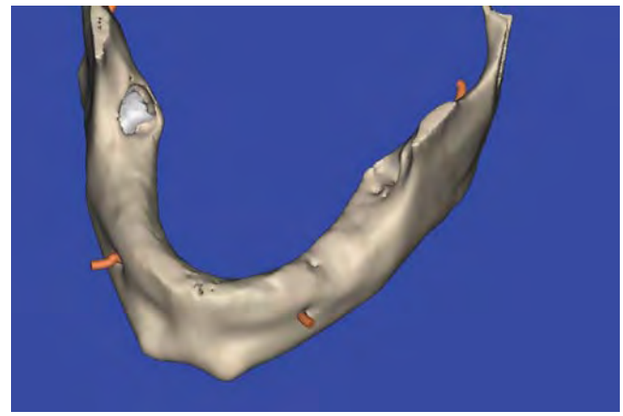

FIGURE 8-54. Assessing the ramus area as a potential donor graft site.

complications. Using advanced software specifically designed for oral surgery applications, different procedures can be simulated including segmental osteotomies and more. Once the dimensions of the donor site have been established, the surgery can be simulated on the three-dimensional model. The donor graft can be virtually removed from the mandible and positioned where it is needed to augment the distant receptor site (Figure 8-56). If the receptor site was part of the three-dimensional reconstructed maxilla, it could be moved to the site to see if it fit properly. This can all be accomplished before touching the scalpel to the patient.

FIGURE 8-55. The cross-sectional view reveals the thickness of the facial cortical plate and the proximity of the inferior alveolar nerve.

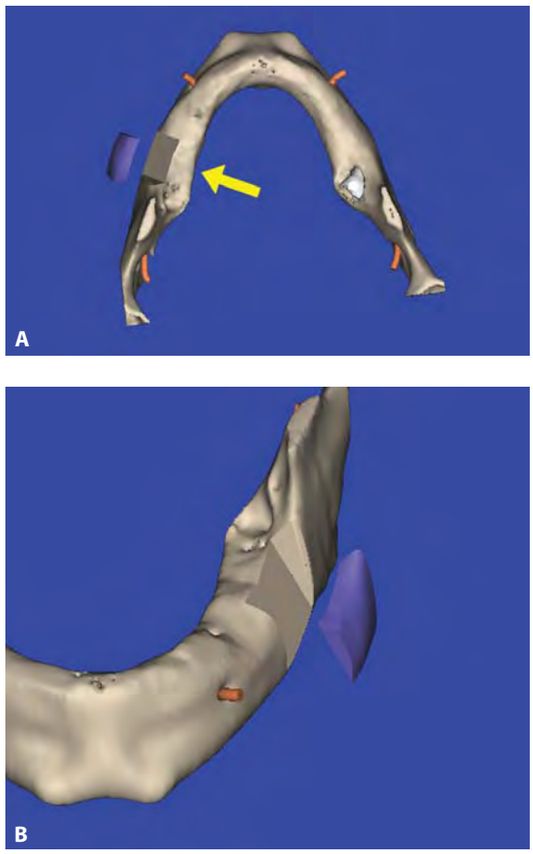

FIGURE 8-56. **A** and **B,** The bone graft of correct dimensions can be virtually "removed" from the donor site and positioned where it is needed to augment the receptor site.

CONCLUSION

It has been well documented that panoramic and periapical radiography are limited in diagnostic accuracy due to the inherent distortion factor, overlap of adjacent structures, the inability to realistically evaluate spatial relationships, assess bone width, or quality. The use of CT/CBCT resolves these issues by accurately supplying undistorted three dimensional assessment of bone width, density, location of nerves, vessels, volume of the maxillary sinus, location of septum, root morphology, the temporomandibular joint complex, spatial position of impacted or supernumerary teeth, and magnitude of potential pathological lesions. The improved diagnostic acuity affords the clinician with the vital information required to formulate and present one or more treatment options to the patient.

The ability to interactively assess patient anatomy with three dimensional imaging has empowered clinicians with an expanded set of tools which can greatly improve diagnostic accuracy. Applications for the use of this technology apply to all specialities of dentistry, but are particularly suited for oral surgery procedures as illustrated in this chapter. The examples are almost limitless as each patient presents with an individual set of anatomical realities which need to be appreciated prior to the development of a definitive treatment plant. Virtual simulation of "routine" extractions can be found to be anything but routine after reviewing the axial or cross-sectional slices of a CT/CBCT scan of the region in question. The shape and dimension of a defect requiring bone grafting can be pre-operatively assessed and visualized in great detail so as to understand the volume required to manage the site, helping to decide between particulate or block grafting techniques. Implant or bone grafting receptor sites can be evaluated for thickness of the buccal or lingual cortex, density of the intermedulary bone, and proximity to vital structures. Manipulation of the 3-D interactive data with new and innovative software tools can yield unprecedented views which allow for inspection of the patient's unique anatomical presentation and provide the means to remove guesswork from the process.

The case examples contained in this chapter were selected to illustrate how three-dimensional imaging and interactive software applications can significantly enhance the diagnosis and treatment planning process through the use of a variety of different applications for the technology. It is important to note that the concepts presented are not limited to specific case types, but provide the potential for expansion into every area of dentaloalveolar surgical, implant, and prosthetic reconstruction. It is the author's opinion that the utilization of CT/CBCT diagnostic imaging by the oral surgeon will significantly impact on the everyday practice workflow including; case presentation, reduction of potential complications, supplemental medical-legal documentation, improved treatment planning capabilities, enhanced communication with referring clinicians, and reduction in patient morbidity during and after the ultimate surgical intervention.

ACKNOWLEDGEMENTS

Thanks to Dr. Richard Kraut, DDS, Chairman, Department of Dentistry, Montefiore Medical Center, Bronx, NY, for his expert surgical treatment and clinical documentation in Case Two.

SUGGESTED READINGS

Alqerban A, Jacobs R, Souza PC, Willems G. In-vitro comparison of 2 cone-beam computed tomography systems and panoramic imaging for detecting simulated canine impaction-induced external root resorption in maxillary lateral incisors. Am J Orthod Dentofacial Orthop. 2009 Dec;136(6):764.e1-11; discussion 764-5.

Amet, E.M. and Ganz, S.D., Functional and Aesthetic Acceptance Prior to Computerized Tomography or Implant Placement. Implant Dentistry, Vol 6, No. 3, Fall 1997;pp193-197.

Angelopoulos C, Aghaloo T. Imaging technology in implant diagnosis. Dent Clin North Am. 2011 Jan;55(1):141-58.

Araryarachkul, P., Caruso, J., Gantes, B., Schulz, E., Riggs, M., Dus, I., Yamada, J. & Crigger, M. Bone density assessments of dental implant sites: 2. Quantitative cone-beam computerized tomography. The International Journal of Oral & Maxillofacial Implants 20: 416–424. 2005

Baqain, Z.H., Karaky, A.A., Sawair, F., Khraisat, A.,Duaibis, R. & Rajab, L.D. (2008) Frequency estimates and risk factors for postoperative morbidity after third molar removal: a prospective cohort study. The International Journal of Oral and Maxillofacial Surgery 66: 2276–2283.

Bedoya MM, Park JH. A review of the diagnosis and management of impacted maxillary canines. J Am Dent Assoc. 2009 Dec;140(12):1485-93. Review.

Berco M, Rigali PH Jr, Miner RM, DeLuca S, Anderson NK, Will LA. Accuracy and reliability of linear cephalometric measurements from cone-beam computed tomography scans of a dry human skull. Am J Orthod Dentofacial Orthop. 2009 Jul;136(1): 17.e1-9; discussion 17-8.

Benington PC, Khambay BS, Ayoub AF. An overview of three-dimensional imaging in dentistry. Dent Update. 2010 Oct;37(8):494-6, 499-500, 503-4 passim.

Boffano P, Ruga E, Gallesio C. Keratocystic odontogenic tumor (odontogenic keratocyst): preliminary retrospective review of epidemiologic, clinical, and radiologic features of 261 lesions from University of Turin. J Oral Maxillofac Surg. 2010 Dec;68(12):2994-9. Epub 2010 Oct 23.

Bornstein MM, Filippi A, Altermatt HJ, Lambrecht JT, Buser D. The odontogenic keratocyst--odontogenic cyst or benign tumor?. Schweiz Monatsschr Zahnmed. 2005;115(2):110-28. Review.

Botticelli S, Verna C, Cattaneo PM, Heidmann J, Melsen B. Two- versus three-dimensional imaging in subjects with unerupted maxillary canines. Eur J Orthod. 2010 Dec 3. [Epub ahead of print]

Capelli M. Autogenous bone graft from the mandibular ramus: a technique for bone augmentation. Int J Periodontics Restorative Dent. 2003 Jun;23(3):277-85.

Caprioglio A, Siani L, Caprioglio C. Guided eruption of palatally impacted canines through combined use of 3-dimensional computerized tomography scans and the easy cuspid device. World J Orthod. 2007 Summer;8(2):109-21. Review.

Chan HL, Misch K, Wang HL. Dental imaging in implant treatment planning. Implant Dent. 2010 Aug;19(4):288-98.

Danza M, Zollino I, Carinci F. Comparison between implants inserted with and without computer planning and custom model coordination. J Craniofac Surg. 2009 Jul;20(4):1086-92.

Di Giacomo, G.A., Cury, P.R., De Araujo, N.S., Sendyk, W.R. & Sendyk, C.L. (2005) Clinical application of stereolithographic surgical guides for implant placement: preliminary results. Journal of Periodontology 76: 503–507.

Dreiseidler T, Mischkowski RA, Neugebauer J, Ritter L, Zöller JE. Comparison of cone-beam imaging with orthopantomography and computerized tomography for assessment in presurgical implant dentistry. Int J Oral Maxillofac Implants. 2009 Mar-Apr;24(2):216-25.

Dula K, Mini R, van der Stelt PF, Buser D. The radiographic assessment of implant patients: decision-making criteria. Int J Oral Maxillofac Implants. 2001 Jan-Feb;16(1):80-9.

Ganz, S.D., The Triangle of Bone - A Formula For Successful Implant Placement and Restoration. The Implant Society, Inc., Vol. 5, No. 2, 1995: 2-6.

Ganz SD. Use Of Stereolithographic Models As Diagnostic and Restorative Aids for Predictable Immediate Loading of Implants. Pract Proced Aesthet Dent 2003; 15(10): 763-771.

Ganz, SD. Presurgical Planning With CT-Derived Fabrication of Surgical Guides. J Oral Maxillofac Surg Vol 63(9), Supplement 2. Sept 2005:59-71.

Ganz, SD. Use of Conventional CT and Cone Beam for Improved Dental Diagnostics and Implant Planning. AADMRT Newsletter, Spring Issue 2005.

Ganz, SD. The Reality of Anatomy and the Triangle of Bone. Inside Dentistry. Vol 2(5) June 2006: pp 72-77.

Ganz, SD, Techniques for the Use of CT Imaging for the Fabrication of Surgical Guides. In: Atlas Oral Maxillofac Surg Clin North Am, Elsevier Saunders 14 (2006) pp 75-97.

Ganz SD. Using interactive technology: "In the Zone with the Triangle of Bone." Dent Implantol Update. 2008 May;19(5): 33-8; quiz p1.

Ganz, SD., Computer-aided Design/Computer-aided Manufacturing Applications Using CT and Cone Beam CT Scan Technology. In Thomas, SL and Angelopoulos C. (ed), Contemporary Dental and Maxillofacial Imaging. Dental Clinics of North America. Philadelphia: Elsevier, Inc., Vol 52(4); 2008: 777-808.

Ganz SD. Restoratively driven implant dentistry utilizing advanced software and CBCT: Realistic abutments and virtual teeth. Dent Today. 2008 Jul;27(7):122, 124, 126-7.

Ganz, SD. "Advanced Case Planning with SimPlant." In Tardieu, P., and Rosenfeld A. (ed) The Art of Computer-Guided Implantology. Chicago: Quintessence, 2009. pp 193-210.

Ganz, SD. "The use of CT/CBCT and interactive virtual treatment planning and the triangle of bone: Defining new paradigms for assessment of implant receptor sites." In: Dental Implants - The Art and Science Ed. Babbush, C. Hahn J., Krauser J, Rosenlicht, J. Saunders. 2010 pp 146-166.

Ganz, SD. Bone Grafting Assessment: Focus on the Anterior and Posterior Maxilla Utilizing Advanced 3-D Imaging Technologies. Dent Implantol Update. June 2009 Vol. 20(6): 41-48.

Ganz, SD. "Implant complications associated with two- and three dimensional diagnostic imaging technologies." In: Dental Implant Complications - Etiology, Prevention, and Treatment. Ed. Froum, SJ. Wiley-Blackwell. 2010 pp 71-99.

Haney E, Gansky SA, Lee JS, Johnson E, Maki K, Miller AJ, Huang JC. Comparative analysis of traditional radiographs and cone-beam computed tomography volumetric images in the diagnosis and treatment planning of maxillary impacted canines. Am J Orthod Dentofacial Orthop. 2010 May;137(5):590-7.

Harris D, Buser D, Dula K, et al. E.A.O. guidelines for the use of diagnostic imaging in implant dentistry. A consensus work-shop organized by the European Association for Osseointegration in Trinity College Dublin. Clin Oral Implants Res 2002;13:566–570.

Hatcher DC, Dial C, Mayorga C. Cone beam CT for pre-surgical assessment of implant sites. J Calif Dent Assoc. 2003 Nov;31(11): 825-33.

Hirsch DL, Garfein ES, Christensen AM, Weimer KA, Saddeh PB, Levine JP. Use of computer-aided design and computer-aided manufacturing to produce orthognathically ideal surgical outcomes: a paradigm shift in head and neck reconstruction. J Oral Maxillofac Surg. 2009 Oct;67(10):2115-22.

Howard-Swirzinski K, Edwards PC, Saini TS, Norton NS. Length and geometric patterns of the greater palatine canal observed in cone beam computed tomography. Int J Dent. 2010;2010. pii: 292753.

Jacotti, M., & Antonelli, P. 3D block technique: from image diagnostics to block graft bone regeneration. Milano, Italy, RC libri. (2005).

Jacotti M. Simplified onlay grafting with a 3-dimensional block technique: a technical note. Int J Oral Maxillofac Implants. 2006 Jul-Aug;21(4):635-9.

Katsnelson A, Flick WG, Susarla S, Tartakovsky JV, Miloro M. Use of panoramic x-ray to determine position of impacted maxillary canines. J Oral Maxillofac Surg. 2010 May;68(5):996-1000.

Laffranchi L, Dalessandri D, Fontana P, Visconti L, Sapelli P. Cone beam computed tomography role in diagnosis and treatment of impacted canine patient's: a case report. Minerva Stomatol. 2010 Jun;59(6):363-76.

Lal, K., White, G.S., Morea, D.N. & Wright, R.F. Use of stereolithographic templates for surgical and prosthodontic implant planning and placement. Part I. The concept. Journal of Prosthodontics 15: 51–58. (2006)

Li TJ. The odontogenic keratocyst: a cyst, or a cystic neoplasm? J Dent Res. 2011 Feb;90(2):133-42.

Madras J, Lapointe H. Keratocystic odontogenic tumour: reclassification of the odontogenic keratocyst from cyst to tumour. J Can Dent Assoc. 2008 Mar;74(2):165-165.

Mandelaris GA, Rosenfeld AL. The expanding influence of computed tomography and the application of computer-guided implantology. Pract Proced Aesthet Dent.2008 Jun;20(5):297-305; quiz 306.

Misch CM. Re: "distance between external cortical bone and mandibular canal for harvesting ramus graft: a human cadaver study". J Periodontol. 2010 Aug;81(8):1103-4; author reply 1104-5.

Misch CM. Autogenous bone: is it still the gold standard? Implant Dent. 2010 Oct;19(5):361.

Mol A, Balasundaram A. In vitro cone beam computed tomography imaging of periodontal bone. Dentomaxillofac Radiol. 2008 Sep;37(6):319-24.

Moreira CR, Sales MA, Lopes PM, Cavalcanti MG. Assessment of linear and angular measurements on three-dimensional cone-beam computed tomographic images. Oral Surg Oral Med Oral Pathol Oral Radiol Endod. 2009 Sep;108(3):430-6.

Morgan TA, Burton CC, Qian F. A retrospective review of treatment of the odontogenic keratocyst. J Oral Maxillofac Surg. 2005 May;63(5):635-9.

Mraiwa N, Jacobs R, van Steenberghe D, Quirynen M. Clinical assessment and surgical implications of anatomic challenges in the anterior mandible. Clin Implant Dent Relat Res. 2003;5(4): 219-25.

Naitoh, M., Hirukawa, A., Katsumata, A. & Ariji, E. Evaluation of voxel values in mandibular cancellous bone: relationship between cone-beam computed tomography and multislice helical computed tomography. Clinical Oral Implants Research 20: 503–506. (2009)

O'Neill R, Al-Hezaimi K. Identification of an odontogenic keratocyst and treatment with guided tissue regeneration: case report. J Can Dent Assoc. 2011 Feb;77:b6.

Orentlicher G, Goldsmith D, Horowitz A. Computer-generated implant planning and surgery: case select. Compend Contin Educ Dent. 2009 Apr;30(3):162-6, 168-73.

Orentlicher G, Goldsmith D, Horowitz A. Applications of 3-dimensional virtual computerized tomography technology in oral and maxillofacial surgery: current therapy. J Oral Maxillofac Surg. 2010 Aug;68(8):1933-59.

Pace R, Cairo F, Giuliani V, Prato LP, Pagavino G. A diagnostic dilemma: endodontic lesion or odontogenic keratocyst? A case presentation. Int Endod J. 2008 Sep;41(9):800-6. Epub 2008 Jul 14.

Rabelo GD, de Paula PM, Rocha FS, Jordão Silva C, Zanetta-Barbosa D. Retrospective study of bone grafting procedures before implant placement. Implant Dent. 2010 Aug;19(4):342-50.

Rodriguez-Recio O, Rodriguez-Recio C, Gallego L, Junquera L. Computed tomography and computer-aided design for locating available palatal bone for grafting: two case reports. Int J Oral Maxillofac Implants. 2010 Jan-Feb;25(1):197-200.

Rosenfeld AL, Mecall RA. The use of interactive computed tomography to predict the esthetic and functional demands of implant-supported prostheses. Compend Contin Educ Dent. 1996 Dec;17(12):1125-8, 1130-2 passim; quiz 1146.

Rosenfeld AL, Mecall RA. Use of prosthesis-generated computed tomographic information for diagnostic and surgical treatment planning. J Esthet Dent. 1998;10(3):132-48.

Roser SM, Ramachandra S, Blair H, Grist W, Carlson GW, Christensen AM, Weimer KA, Steed MB. The accuracy of virtual surgical planning in free fibula mandibular reconstruction: comparison of planned and final results. J Oral Maxillofac Surg. 2010 Nov;68(11):2824-32. Epub 2010 Sep 9.

Rothman, Stephen L.G. Computerized Tomography of the Enhanced Alveolar Ridge. In: Dental Applications of Computerized Tomography, Chicago. Quintessence Publishing Co., Inc.1998:pp 87–112.

Sarment, D.P., Shammari, K., & Kazor, C.E. Stereolithographic surgical templates for placement of dental implants in complex cases. Int J Periodontics Restorative Dent 2003 23:287-295.

Sharif FNj, Oliver R, Sweet C, Sharif MO. Interventions for the treatment of keratocystic odontogenic tumours (KCOT, odontogenic keratocysts (OKC)). Cochrane Database Syst Rev. 2010 Sep 8;(9):CD008464. Review.

Simon JH, Enciso R, Malfaz JM, Roges R, Bailey_Perry M, Patel A. Differential diagnosis of large periapical lesions using cone-beam computed tomography measurements and biopsy. J Endod. 2006 Sep;32(9):833-7. Epub 2006 Jul 7.

Tonetti MS, Hämmerle CH; European Workshop on Periodontology Group C. Advances in bone augmentation to enable dental implant placement: Consensus Report of the

Sixth European Workshop on Periodontology. J Clin Periodontol. 2008 Sep;35(8 Suppl):168-72.

Van Steenberghe D. Interactive imaging for implant planning. J Oral Maxillofac Surg. 2005 Jun;63(6):883-4.

Wood, D.L., Hoag, P.M., Donnenfeld, O.W. & Rosenfeld, L.D. (1972) Alveolar crest reduction following full and partial thickness flaps. Journal of Periodontology 43: 141–144.

Worthington P, Rubenstein J, Hatcher DC. The role of cone-beam computed tomography in the planning and placement of implants. J Am Dent Assoc. 2010 Oct;141 Suppl 3:19S-24S.

Zhao YF, Wei JX, Wang SP. Treatment of odontogenic keratocysts: a follow-up of 255 Chinese patients. Oral Surg Oral Med Oral Pathol Oral Radiol Endod. 2002 Aug;94(2):151-6.